

Review

Responsive DNA Nanostructures for Bioanalysis and Therapy

Yingfei Wang ^{1,†}, Yue Zhang ^{2,†} , Huangxian Ju ¹ and Ying Liu ^{1,3,*} 

¹ State Key Laboratory of Analytical Chemistry for Life Science, School of Chemistry and Chemical Engineering, Nanjing University, Nanjing 210023, China; 18168012632@163.com (Y.W.); hxju@nju.edu.cn (H.J.)

² School of Pharmacy, Nanjing University of Chinese Medicine, Nanjing 210023, China; zhangyue035@njucm.edu.cn

³ Chemistry and Biomedicine Innovation Center, Nanjing University, Nanjing 210023, China

* Correspondence: yingliu@nju.edu.cn

† These authors contributed equally to this work.

Abstract: DNA nanostructures have been widely explored as an encouraging tool for bioanalysis and cancer therapy due to its structural programmability and good biocompatibility. The incorporation of stimulus-responsive modules enables the accurate targeting and flexible control of structure and morphology, which is benefit to precise bioanalysis and therapy. This mini review briefly discusses the advancements in stimuli-responsive DNA nanostructures construction and their applications in biomolecules sensing and cancer treatment.

Keywords: DNA nanostructures; stimuli-responsive; bioanalysis; imaging; therapy

1. Introduction

DNA nanostructures, which are formed through the self-assembly of DNA strands, have won considerable attention and become a breakthrough in nanotechnology. By leveraging the principles of Watson–Crick base pairing, individual DNA strands are meticulously programmed to predetermined shapes with various functions such as sensing and therapeutic applications [1–4]. As a natural component of all living organisms, DNA has inherently superior biocompatibility, which reduces the risk of adverse reactions in biological systems. Additionally, DNA structures with multifarious configurations could be easily obtained using techniques such as DNA origami, which offers a simple method to fold long single strands into desired shapes through self-assembly with staple strands, and larger assemblies could be further established from individual DNA structures [5]. More importantly, it is convenient to functionalize DNA nanostructures with various biomolecules [6–8]. These unique properties endow DNA structures with great power and make them a promising tool in biological applications.

When applying DNA nanostructures in biological systems, the complexity of in vivo environment impairs application efficiency. On one hand, biomarkers, as detection targets, are usually in low expression levels in biological environments; therefore, specific and efficient DNA cascade reactions are required to be embedded in DNA nanostructures [9–11] to enhance target responsiveness and improve detection sensitivity or therapeutic efficacy. On the other hand, the diffused distribution of biomarkers out of target position may result in the “nonselective” activation of DNA nanostructure and cause “false-positive” signals in diagnosis and side effect in therapy [12–14]. Therefore, responsive DNA nanostructures that are sensitive to biological endogenous factors or external applied stimuli have been designed with spatiotemporal regulation of their structure and motion for bioimaging [15–17] or precise therapy [18–20].

Stimuli that trigger the transformation of DNA nanostructures includes external factors (such as light [21–23], temperature [24–26], or magnetic field [27–29]) and internal factors (such as acidity [30,31], small molecules [32–34], nucleic acids [35–37], or proteins [35,38,39]). In response to stimuli activation, the programmed DNA nanostructures would generate



Citation: Wang, Y.; Zhang, Y.; Ju, H.; Liu, Y. Responsive DNA Nanostructures for Bioanalysis and Therapy. *Chemistry* **2023**, *5*, 2182–2204. <https://doi.org/10.3390/chemistry5040147>

Academic Editor: Di Li

Received: 30 June 2023

Revised: 6 October 2023

Accepted: 7 October 2023

Published: 13 October 2023



Copyright: © 2023 by the authors. Licensee MDPI, Basel, Switzerland. This article is an open access article distributed under the terms and conditions of the Creative Commons Attribution (CC BY) license (<https://creativecommons.org/licenses/by/4.0/>).

optical or electrical signals or release cargoes through specific conformational changes or bond breaks. Elaborate designs of configuration reversal to switch between different conformations allow for dynamic control over the functions of DNA nanostructures. This property has been widely utilized in applications such as molecular switches or logic gates for bioanalysis [40–43]. Additionally, cascade reactions, including DNAzyme reactions, hybridization chain reaction, and DNA walkers, involve a series of sequential reactions that can be programmed into DNA nanostructures [44–46]. These reactions can be triggered by specific stimuli and lead to a cascade of events for the amplification of desired response and signals, which are especially essential for applications that require signal amplification or complex molecular computations.

Stimuli-responsive DNA nanostructures offer a versatile platform for achieving controlled and specific responses to various stimuli. By harnessing these responses, researchers can develop innovative applications in areas such as biosensing, drug delivery, and precision medicine. In this review, we discussed the exciting advancements in the field of stimuli-responsive DNA nanostructures and their potential applications in bioanalysis and therapy. As our understanding of DNA nanotechnology advances, we can expect to see further developments in the design and utilization of responsive DNA nanostructures for a wide range of biomedical applications.

2. Responsive DNA Nanostructures for Biosensing and Bioimaging

Developing biosensing and bioimaging strategies is important to report the occurrence and development of diseases, guide treatment, and evaluate therapeutic results. DNA nanostructures for biosensing and bioimaging are usually composed of recognition segments (such as DNAzymes, i-motif, G-quadruplex, and aptamers et al.) that exhibit high recognition ability towards specific biomarkers and signaling segments that demonstrated measurable signal change. The recognition events of the DNA nanostructure to targets act as stimuli, resulting in their configuration change with a correspondingly detectable signal. There are two key points to keep in mind when designing a responsive DNA nanostructure for biosensing/bioimaging: amplifying signals from lowly expressed detection targets and suppressing “false positive” signals from the nonspecific activation of the DNA nanostructure.

2.1. DNA Nanostructures for Detection Signal Amplification

The precise detection of biomarkers is significant for clinical diagnosis accuracy. However, many biomarkers are usually low in abundance and require highly effective enrichment and signal amplification strategies for detection. Smart responsive DNA nanostructures can not only offer specific recognition to detection targets but also amplify detection signals by nucleic acid cascade reactions, which have been applied for multiple detection targets including miRNAs, extracellular vesicles, and circulating tumor cells. The following will address advances toward the development of smart responsive DNA nanostructures for detection signal amplification.

2.1.1. In Vivo miRNAs Detection

MicroRNAs (miRNAs) are endogenous non-coding RNAs, which participate in many physiological processes, including cells proliferation, differentiation, apoptosis and stress responses [47–49]. Aberrant expression of miRNAs usually relates to cancer occurrence and progression, making it a potential biomarker for clinical diagnosis and disease treatment [50]. However, their short length, low abundance and high similarity among homogeneous sequence make miRNAs detection challenging. Nonenzymatic catalytic amplification strategies based on DNA cascade reactions, such as hybridization chain reaction (HCR) and catalytic hybridization assembly (CHA), and enzymatic rolling circle amplification (RCA), have been widely applied as signal amplification techniques for sensitive miRNAs detection.

Circulating miRNAs exist in various body fluids and emerge as a useful diagnostic biomarker for a variety of diseases such as malignancy, cardiovascular, neurologic, and metabolic diseases [51–53]. Besides their naturally low abundance in body fluids, one of the main challenges for circulating miRNAs detection is that they usually exist within protein complexes, and therefore require a pretreatment process to be released from the protein complex before detection. To solve this problem, Doyle et al. treated raw serum samples with SDS and RNase inhibitors to release target miRNAs from protein complexes, and realized the direct detection of unprocessed human serum samples using a nonfouling PEG hydrogel particle substrate (Figure 1A) [54]. The hydrogel particles were modified with capture probes, which recognized target miRNA-141 and enabled subsequent rolling circle amplification reactions with subsequent fluorescent reporters labelling for signal amplification. The SDS treatment, the antifouling property of hydrogel particles, and the contribution of DNA cascade reactions to signal amplification ensured the direct detection of target miRNAs in small quantities of unprocessed human serum samples without the need for RNA extraction. However, such enzymatic catalytic isothermal DNA amplification strategies require strict reaction conditions of enzymes, which hampered their application in clinic diagnostics. Liu et al. designed a fluorescent hydrogel array for the high-throughput detection of miRNA-21 based on the integration of miRNA-21-responsive DNA hybridization chain reaction (HCR) with interfacial cation exchange amplification (Figure 1B) [55]. After the capture of target miRNA-21 in a hydrogel array via hybridization with capture probes, HCR, independent of enzyme participation, was performed in the hydrogel for signal amplification. HCR products were further labelled with CdS quantum dots, which demonstrated strong fluorescence signal via a cation exchange reaction for sensitive quantification of target miRNA-21. After the cation exchange reaction, Cd^{2+} was released from CdS quantum dots and distributed in the hydrogel, which formed a product with dye Rhod-5N and demonstrated strong fluorescence to further enhance the miRNA detection signal. This method demonstrated great performance in the direct quantification of miRNA-21 from crude cancer cell lysates and clinical serum samples.

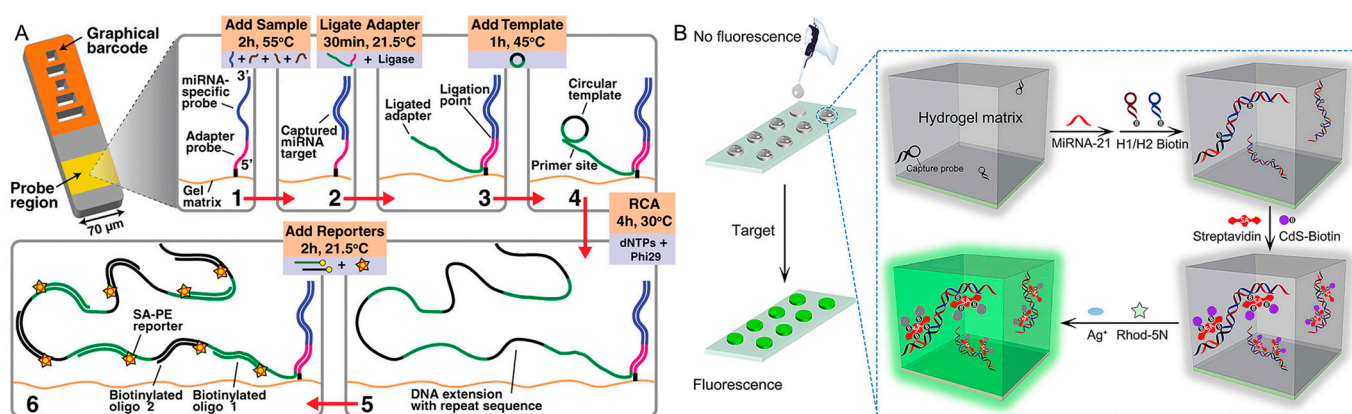


Figure 1. (A) Morphologically encoded non-fouling hydrogel particles for multiplex miRNAs detection with RCA [54]. Reproduced with permission from Anal. Chem., published by American Chemical Society, 2011. (B) Fluorescent hydrogel array for miRNA-21 detection based on HCR coupled with interfacial cation exchange amplification [55]. Reproduced with permission from Anal. Chim. Acta, published by Elsevier B.V., 2019.

Besides circulating miRNAs, self-assembled DNA nanostructures were also widely utilized to quantitatively analyze miRNAs at the single-cell level. Chen et al. performed DNA catalytic hairpin assembly reaction within a picoliter droplet, and achieved single-cell miRNA-21 quantification in different breast cancer cell lines (Figure 2A) [56]. This method provided a powerful tool for rapid and precise biomedical quantitative detection. Furthermore, Tang et al. proposed a DNA cascade reaction-based quadratic isothermal

amplification strategy for multiple microRNAs profiling at the single-cell level, and realized human cancer identification (Figure 2B) [57]. They performed single-cell miRNAs analysis in water-in-oil droplets that synthesized with microfluidic technology. Single cells were encapsulated in individual droplets with DNA amplifiers for quadratic isothermal amplification, which reduced target miRNAs degradation and confined fluorescent amplified products in pico-liter space for signal enhancement. The resulting fluorescent signals were collected by a multi-color fluorescence detector. This single-cell multiple miRNAs analysis method indicated potential application in differentiation and identification of tumors. Furthermore, Liu et al. designed a hydrogel microbead for single cell encapsulation and achieved simultaneous quantification of multiplexed miRNAs by coupling with catalytic hairpin assembly (CHA) and rolling circle amplification (RCA) (Figure 2C) [58]. Hydrogel microbead provided similar hydrous microenvironment to maintain the function of DNA nanostructures and its porous structure enabled the free diffusion of DNA amplification reaction strands and ease removal of unreacted DNA strands. Single-cell encapsulated hydrogel microbeads were fabricated with a flow focusing configured microfluidic chip and functionalized with target miRNAs capture probes. Fluorescent dye-labelled DNA strands were then hybridized with DNA cascade reactions products for different miRNAs quantifications. HepG2, HCCLM3, MHCC-97L, and HHL-5 cell lines were screened and showed distinct miRNAs profiles, demonstrating the promising identification of cancer cell types via effectively simultaneous quantification of multiple miRNAs. Therefore, multiplexed miRNAs expression at single-cell levels contributed to cell heterogeneity exploration and cell subtype discrimination.

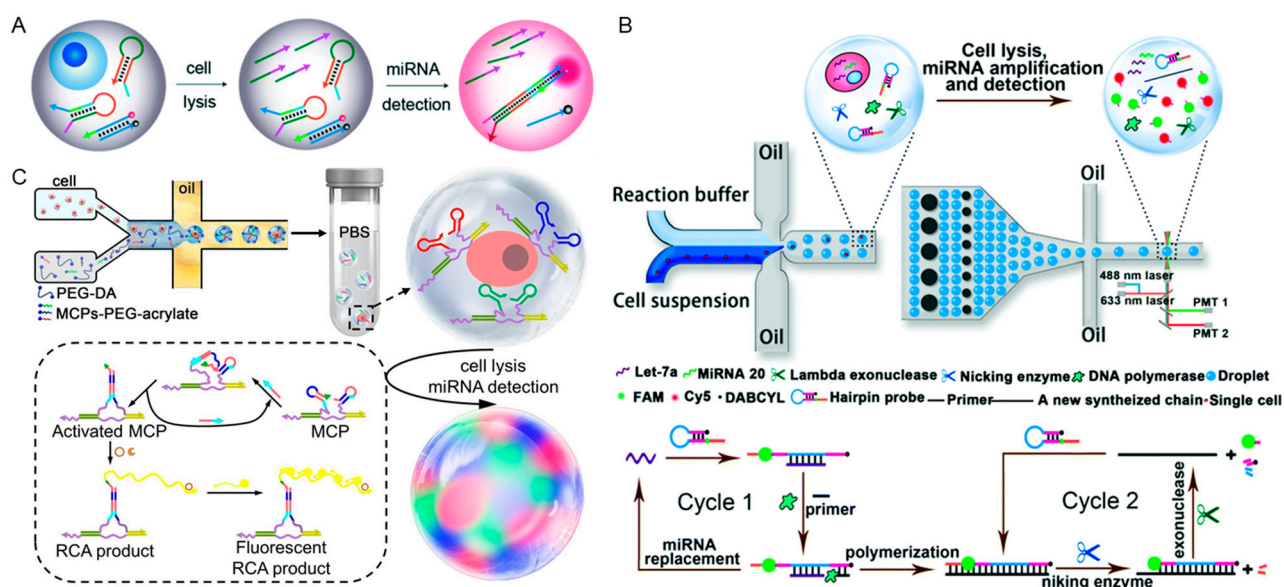


Figure 2. (A) Hairpin DNA isothermal amplifier for the catalytic signal enhancement of miRNA-21 expression in a single cell [56]. Reproduced with permission from Lab Chip, published by The Royal Society of Chemistry, 2018. (B) Quadratic isothermal amplification for single-cell miRNAs analysis in water-in-oil droplets [57]. Reproduced with permission from ChemComm, published by The Royal Society of Chemistry, 2019. (C) Single-cell multi-miRNAs quantification by DNA cascade amplifications in hydrogel microbeads for cell subtype discrimination [58]. Reproduced with permission from Chem. Sci., published by The Royal Society of Chemistry, 2022.

2.1.2. Extracellular Vesicles Detection

Extracellular vesicles (EVs) are lipid bilayer confined particles that are naturally secreted from almost all types of cells and found to circulate through many different body fluids [59,60]. Tumor cells related EVs contain cancer-related information and participate in intracellular communication and pathological processes [61], which makes them a po-

tential biomarker for cancer diagnosis. However, the small size (30–200 nm) of EVs and low expression of surface biomarkers result in detection difficulty. DNA-based signal amplification technologies are widely utilized to improve detection sensitivity. Taking advantage of target-initiated DNA cascade reactions on the EVs' membrane, Zhong et al. realized the visualization of a single extracellular vesicle via traditional flow cytometry and revealed the heterogeneity of EVs (Figure 3A) [62]. To perform target-initiated signal amplification, a conformation-switchable DNA probe was designed to recognize CD63, which is a surface protein marker in various EVs. Upon target recognition, the DNA probe changed its configuration and exposed toehold to initiate HCR on the vesicle membrane. The resulting fluorescent HCR products not only increased the physical size of a single EV, but also amplified the signal for surface biomarkers with low expression, enabling the visualization of single EVs in a conventional flow cytometer. Li et al. developed an electrochemical detection strategy based on DNA cascade signal amplification reaction on vesicle membrane (Figure 3B) [63]. Aptamer-modified magnetic beads which recognize EVs membrane proteins CD63 and EpCAM were anchored on EVs surface for magnetic separation. Cholesterol functionalized primer strands were anchored into the EVs membrane via hydrophobic interaction to form SNAs and subsequently extended to a polyT strand. Methylene blue (MB) group, as the electroactive molecule, was modified on a polyA DNA strand and hybridized with a polyT DNA strand for signal amplification. The as-obtained polyT-A hybrid was then cleaved by Exo III and released the polyA strand from the substrate. The released polyA strand (MB functionalized) was collected on an electrode to obtain an electrochemical signal and achieved quantitative EVs detection.

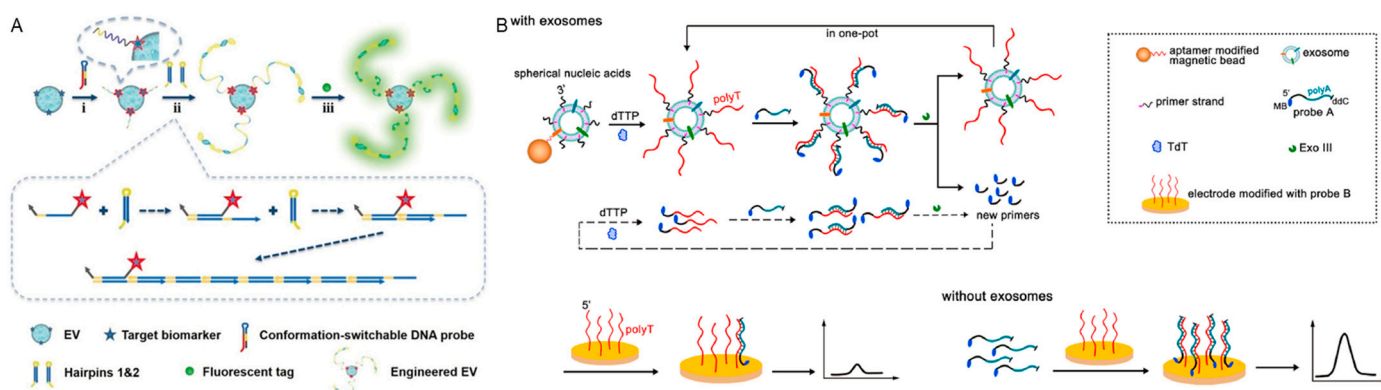


Figure 3. (A) Target-initiated engineering of DNA nanostructures enabled flow cytometry analysis of single extracellular vesicles [62]. (i) Probe conformation change upon target recognition, (ii) DNA hybridization cascade, (iii) fluorescent tag labelling. Reproduced with permission from *Angew. Chem. Int. Ed.*, published by Wiley, 2018. (B) electrochemical detection of EVs based on responsive SNAs [63]. Reproduced with permission from *Biosens. Bioelectron.*, published by Elsevier B.V., 2021.

2.1.3. Circulating Tumor Cells Detection

Circulating tumor cells (CTCs) were discovered in 1869 for the first time. They are tumor cells that have sloughed off from solid tumors and circulate in the blood, representing a real-time snapshot of solid tumors [64]. CTCs carry a variety of information concerning tumor immunophenotype, genome, transcriptome, protein expression, tumor heterogeneity, etc., which facilitate tumor early screening, therapy, recurrence monitoring, and prognosis assessment, and have thus attracted considerable attention from researchers and clinicians in the past few decades [65]. In 2004, the U.S. Food and Drug Administration (FDA) approved “CellSearch system” as a diagnostic tool for CTC detection to predict progression-free survival and overall survival in patients with metastatic breast cancers. In 2012, the China Food and Drug Administration (CFDA) granted the first CTC diagnostic system for clinical application. In 2017, “Cell Collector” was further cleared by the CFDA for in vivo CTC diagnostics. In 2019, CTCs were officially listed as a clinical biomarker to

evaluate therapeutic effects in the Chinese Guideline on the CSCO Breast Cancer Guidelines. Despite the progress in CTC-based bioanalysis since their discovery, their precise detection is still challenging due to the extreme rarity, inherent heterogeneity, and the complex whole blood matrix. Thus, efficient and specific isolation and enrichment of CTCs are usually required as pretreatment techniques. DNA nanostructures contain aptamers that target specific CTC membrane molecules for CTC capture and screening. The affinity of aptamers determines their recognition and binding capability for CTCs, which affects the capture efficiency and detection sensitivity. Li et al. proposed an electrochemical method for the direct analysis of CTCs in whole blood by coupling DNA nanostructures with HCR (Figure 4A) [66]. EpCAM, one of the CTCs membrane protein was recognized by a hairpin structure DNA strand, and subsequently initiated the HCR process to form a DNA nanostructure on the CTC surface and bring the two originally separated segments of the G-quadruplex sequence into close proximity. Thiol group functionalized tetrahedral DNA nanostructures were immobilized onto a Au electrode and acted as hunters to capture CTCs with the as-formed DNA structure. Hemin molecules were added in and reacted with repeated G-quadruplex in the HCR products to form G-quadruplex/hemin complexes as an electroactive molecule for the direct electrochemical analysis of rare CTCs. This strategy achieved an ultralow detection limit as a couple of cells mL^{-1} and linear range from 10 to 10^4 cells mL^{-1} , indicating its advantages in monitoring rare cells.

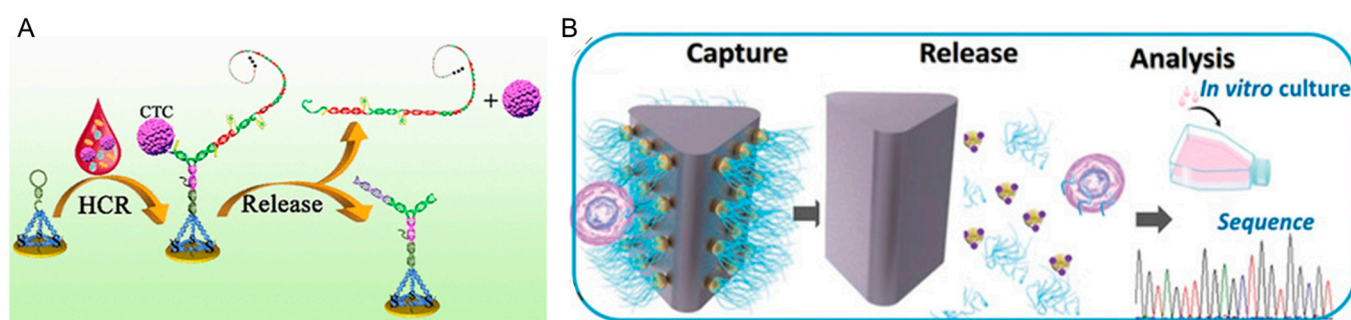


Figure 4. (A) Direct analysis of CTCs on the responsive DNA nanostructures functionalized electrode surface [66]. Reproduced with permission from *Anal. Chem.*, published by American Chemical Society, 2020. (B) Nanointerfaces with multivalent aptamers as recognition elements for CTCs [67]. Reproduced with permission from *Angew. Chem. Int. Ed.*, published by Wiley, 2019.

Compared with monovalent aptamers, multivalent aptamers were also applied to enhance binding affinity to CTCs. Yang and his coworkers have made a great progress toward capturing and releasing CTCs in a controllable approach using DNA nanostructures with multivalent recognition elements [67–69]. They engineered a deterministic lateral displacement (DLD)-patterned microfluidic chip modified with multivalent aptamer-functionalized gold nanoparticles to enhance CTCs capture efficiency (Figure 4B). The multivalent aptamer enhanced CTCs capture efficiency by more than 300% compared with a monovalent aptamer. Moreover, the captured CTCs were released through a thiol exchange reaction with up to 80% release efficiency and 96% of cell viability, which facilitated downstream CTCs culture and analysis [67].

2.2. DNA Nanostructures against False-Positive Detection Signal

DNA nanostructures have been widely used for intracellular bioimaging for their high programmability, ease of synthesis, and good biocompatibility. Wang et al. developed a series of DNA nanostructures via construction of a cascade DNA amplification circuit for reliable cancer cell discrimination and *in vivo* bioimaging [70–75]. For example, inspired by the self-reproducing growth of dandelions, they engineered a stimuli-responsive auto-catalytic hybridization assembly (AHA) circuit through the autonomous cross-initiation of cascade hybridization reaction (CHR) and catalytic DNA assembly (CDA) (Figure 5A). The

initiator, I, (dandelion seed) initiated the generation of stick-like CHR nanowires where the tandem, T, catalyzed the assembly of numerous CDA products bearing newly exposed I analogs (dandelion seeds). Then, the released I analog continuously motivated the autonomous cross-activation of CHR and CDA constitutes of AHA circuit, which gave rise to the accumulation of new initiators and progressive reaction acceleration in a certain space for unlimited exponential signal amplification that enabled the accurate imaging of miRNA from living cells and mice [72].

Though demonstrating an impressive capability to amplify signals from low-abundance biomarkers, the further application of smart responsive DNA nanostructures for precise intracellular biomarkers imaging still faces the following challenges: (1) the “always active” design of most DNA nanostructures makes them susceptible to extracellular targeting in the tumor microenvironment or serum, which would cause nonspecific fluorescence signal amplification before intracellular delivery and result in a false positive signal; (2) the different cells uptake efficiency would also contribute to intracellular signal differences due to the “absolute intensity-dependent” mode with a single luminance channel for signal acquisition. Both of these factors impair the detection accuracy.

Only having target specificity is not enough for precise imaging, since the as-obtained DNA nanostructures not only responded to the detection target at the tumor position but also to target molecules that diffused in systematic circulation out of the tumor position. This would inevitably result in inaccurate detection and high background noise in images due to nonspecific extracellular activation. DNA nanostructures with the capability of controllable activation contributed to the elimination of the false positive signal. Lu et al. designed a light-regulated aptamer biosensor responsive to ATP and realized the spatiotemporal controlled imaging of mitochondrial ATP in living cells [76]. The recognition of aptamer to ATP was blocked by a photo-cleavable (PC) strand and loaded onto a dequalinium-based liposome-like vesicle (DQAsome), which targeted mitochondria. When it reached the mitochondria, the PC strand complementary to ATP aptamer was cut upon 365 nm ultraviolet light irradiation and the corresponding ATP recognition resulted in intracellular fluorescence recovery. Although UV-activated probes improved the spatiotemporal precision for bioimaging, poor tissue penetration and phototoxicity of UV light limited their further in vivo application. Upconversion nanoparticles (UCNPs) are capable of converting near-infra-red (NIR) excitation into visible and ultraviolet emissions, which benefits cell bioimaging with deep tissue penetration, excellent photostability, and low phototoxicity [77]. By coupling with DNA nanodevices, UCNPs act as energy transducers, and transfer NIR excitation to UV emission for photoactivation of DNA nanostructures. Li et al. developed a novel DNA nanodevice by combining a photoactivatable DNA probe with UCNPs for NIR light-activated spatiotemporal imaging of intracellular miRNA (Figure 5B) [78]. A photocleavable linker was incorporated into the hairpin loop of a molecule beacon, which blocked the target miRNA recognition region. UCNPs acted as the NIR-to-UV transducers, and upon NIR light irradiation, UCNPs emitted UV light, which caused the photolysis of the PC linker and enabled dose-dependent displacement of the quencher-labeled strand in the cleaved PBs, resulting in a significant fluorescent signal increase. UCNPs also acted as the carrier for DNA strands loading and delivery, which enhanced the intracellular delivery efficiency of negatively charged DNA strands. This NIR light activated the miRNA sensing strategy and achieved successful cancer-specific bioimaging both in vitro and in vivo.

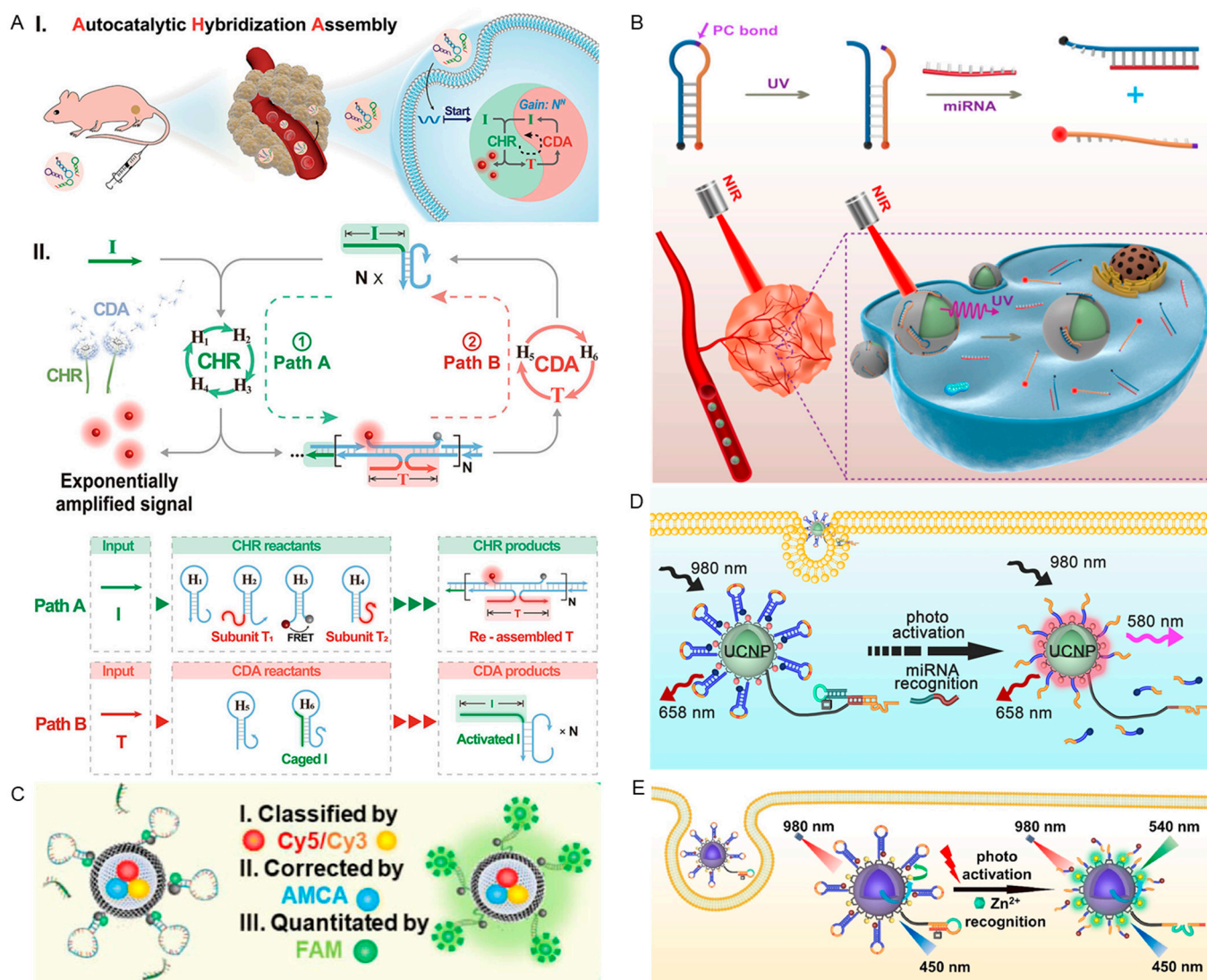


Figure 5. (A) An autocatalytic hybridization assembly circuit engineered by the autonomous cross-initiation of cascade hybridization reaction (CHR) and catalytic DNA assembly (CDA) for amplified *in vivo* miRNA imaging [72]. (I) *In vivo* imaging of miRNA based on the AHA strategy, (II) Principle of the AHA for exponentially amplified detection of target nucleic acid using enzyme-free autocatalytic hybridization assembly (AHA) circuit. Reproduced with permission from *Angew. Chem. Int. Ed.*, published by Wiley, 2022. (B) A NIR-light-activated DNA probe for spatiotemporal control imaging of intracellular miRNA [78]. Reproduced with permission from *J. Am. Chem. Soc.*, published by American Chemical Society, 2019. (C) FluoELs modified with molecular beacon detection probes for multiplexed miRNA detection [79]. Reproduced with permission from *Angew. Chem. Int. Ed.*, published by Wiley, 2022. (D) A UV-light-activated DNA machine with an internal standard for precise intracellular miRNA imaging [80]. Reproduced with permission from *Chem. Sci.*, published by The Royal Society of Chemistry, 2020. (E) A NIR-light-activatable DNA nanomachine with an internal standard for the accurate intracellular imaging of Zn^{2+} [81]. Reproduced with permission from *Anal. Chim. Acta*, published by Elsevier B.V., 2022.

To correct the false positive signals caused by the cellular uptake variation of different cells, Dong et al. proposed a robust combinatorial fluorescence-encoding method to quantify multiplexed miRNAs in a single living cell, termed fluorophores-encoded error-corrected labels (FluoELs) (Figure 5C). The FluoELs were prepared by proportionally embedded Cy3 and Cy5 in the mesoporous silica nanoparticles (MSNs) for FL encoding and the same amount of AMCA fluorophores for error correction. The as-obtained FluoELs

were modified with molecular beacon detection probes for the simultaneous imaging of multiple miRNAs in individual living cell and facilitated evaluation of miRNA expression profiles [79]. In addition, the multiple luminescence emissions of UCNPs under NIR light excitation offer an opportunity for the self-correction of intracellular bioimaging. Liu et al. presented a photo zipper locked DNA nanomachine based on Er-doped UCNPs with an internal standard, and applied it for precise miRNA imaging in living cells (Figure 5D) [80]. The DNA nanomachine was constructed by simultaneously connecting the DNAzyme walker hybrid with a photo zipper, the corresponding substrate strands, and Cy3 as an energy transducer on UCNPs surface. The miRNA recognition area was blocked effectively with the exquisitely designed photo zipper to protect the DNA nanomachine from extracellular activation during cell delivery. After NIR activation, DNA nanomachine responded to miRNA in living cells to produce significant fluorescence amplification for the highly sensitive imaging of intracellular miRNA. Taking advantage of the multiple luminescence emissions of UCNPs, imaging internal standard was chosen as the unchanged emission at 658 nm for self-correction of Cy3 fluorescence to achieve ratiometric detection. This strategy would have broad applications in the detection of other biomarkers. Furthermore, Liu et al. designed a NIR light activatable P-DNA nanomachine based on Tm-doped UCNPs with an internal standard, and achieved the accurate intracellular imaging of Zn^{2+} (Figure 5E) [81]. The P-DNA nanomachine was constructed by FITC modified UCNPs, photo-locked DNAzyme strand and its corresponding substrate strands labelled with BHQ1. In addition, 980 nm NIR light excitation was transduced to 365 nm emission for photolysis of PC linker and activation of DNAzyme walker. The unchanged emission at 450 nm worked as internal standard to improve the detection accuracy, while the 980 nm activated DNA walker responded to Zn^{2+} and cleaved the BHQ1 labelled substrates, resulting in FITC fluorescence recovery at 540 nm. This method achieved accurate Zn^{2+} sensing in living cells.

3. Smart Responsive DNA Nanostructures for Therapy

The flexibility of the structure design with convenience for chemical modification further extends the application of DNA nanomachines to drug delivery and disease treatment. The following will describe several typical DNA nanostructures with different response mechanisms for the application of cancer therapy.

3.1. Response to Small Molecules

3.1.1. pH

Intracellular pH plays a vitally important role in the cellular metabolism as well as the proliferation and apoptosis of cells. The endosomes and lysosomes, which participate in the endocytic process of nanoparticles, exhibit a relatively low pH ranging from 4.5 to 6.5 [82]. Moreover, cancer cells and the tumor microenvironment mostly have a lower pH (6.5 to 4.5) in comparison with normal cells and organs, which provides an afflatus for the precise targeted delivery of drugs [83]. Willner et al. designed a pH-responsive delivery system based on DNA i-motif structures (Figure 6A) [84]. In this study, UiO-66 metal organic framework nanoparticles NMOFs were proposed, which are locked by DNA tetrahedral gates to load doxorubicin (Dox). At acidic pH, the gated tetrahedra dissociates with NMOFs through the formation of the i-motif structure, which led to NMOFs unlocking and drug release. Additionally, AS1411 aptamer was used for the targeting of cancer cells through its combination with overexpressed nucleolin receptors. Ding et al. created a vaccine based on DNA nanodevices for cancer immunotherapy. By accurately assembling antigens and multiple adjuvants within the inner cavity of a tubular DNA nanostructures, adjuvants and antigens are released in a pH-responsive manner, and the purpose of efficient co-delivery and controlled release of multiple therapeutic cargoes is realized [85].

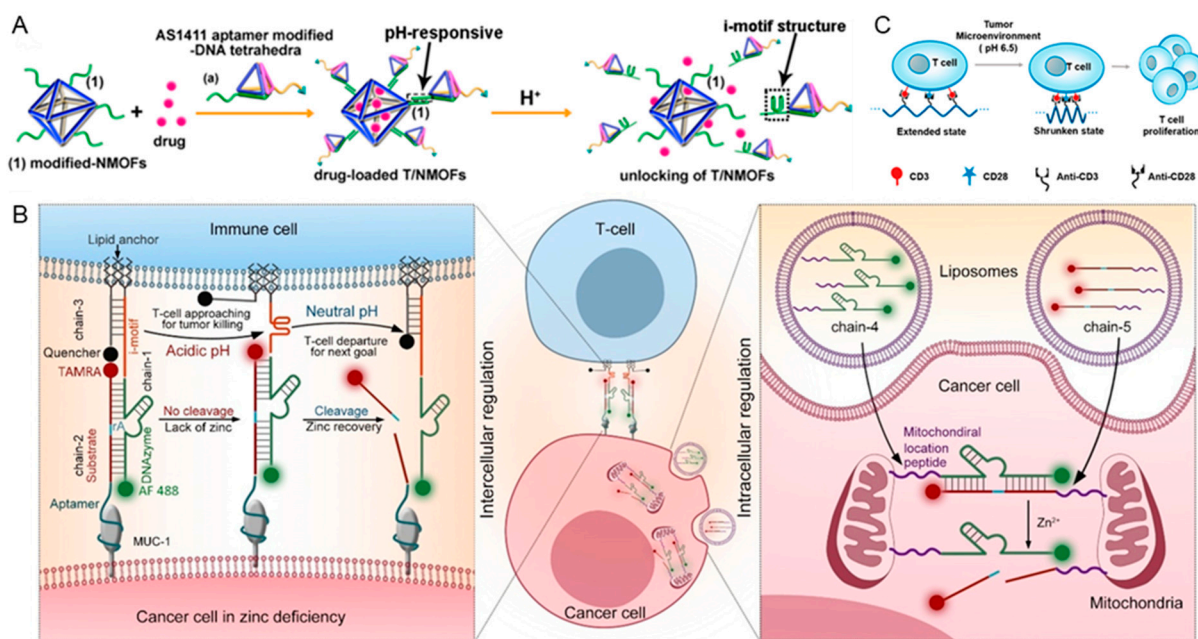


Figure 6. (A) Assembly of the DOX-loaded T/NMOF hybrids and the pH-induced release of the loads [84]. Reproduced with permission from ACS Nano, published by American Chemical Society, 2021. (B) Molecular machines based on engineering DNAzyme and pH-induced interactions between T Cells and cancer cells [86]. Reproduced with permission from Angew. Chem. Int. Ed., published by Wiley, 2022. (C) pH-driven iDNS for in vivo activation of T-cell proliferation [87]. Reproduced with permission from Nano Lett., published by American Chemical Society, 2022.

Taking advantage of the relatively low pH value (pH 6.5) in the tumor microenvironment, responsive therapeutic strategies have been developed. Lu et al. designed an engineered DNAzyme molecular machine based on pH change to regulate the i-motif structure (Figure 6B) [86], in which the i-motif is folded under the acidic tumor microenvironment to shorten the distance between cells. Subsequently, the release of T cells from cancer cells was achieved through DNAzyme cleavage in the presence of metal ions Zn²⁺. This strategy contributed to the dynamical regulation of T cell/cancer cell interactions.

Shi et al. designed a pH-responsive interlocked DNA nano-spring (iDNS) to specifically activate T-cell proliferation for antitumor immunotherapy (Figure 6C) [87]. The lower pH value in the solid tumor drove the springlike shrinking of the interlocked structure of iDNS, which possessed a more rigid scaffold for the precise control of the spatial distribution of ligands. This iDNS achieved accurate regulation of the nanoscale distribution of receptors on the T cell surface, generating significant T-cell proliferation for the enhanced antitumor immunotherapy efficacy.

3.1.2. ATP

5'-adenosine triphosphate (ATP) is one of the most abundant physiological molecules in cells as a coenzyme, and has been used as a new trigger for drug delivery. Gu et al. used ATP as a trigger for the controlled release of anticancer drugs. The designed nano gel is mainly composed of three different functional components: ATP-responsive DNA motif with doxorubicin (Dox) and protamine and hyaluronic acid (HA) cross-linked shell (Figure 7A). Anionic HA is encapsulated in the core complex to form a protective shell and also supports active tumor targeting. After intravenous injection, nano gel accumulated at tumor sites due to passive and active targeting. HAase degraded HA shell, exposed the complex of protamine and Dox-inserted double-stranded bodies (Dox/double stranded bodies). The protamine component promoted endosome escape, and enabled the effective transport of Dox/Duplex into cytosol. ATP-responsive Dox/Duplex dissociation

resulted in effective release of Dox, which eventually accumulates in the nucleus to produce cytotoxicity and apoptosis [88].

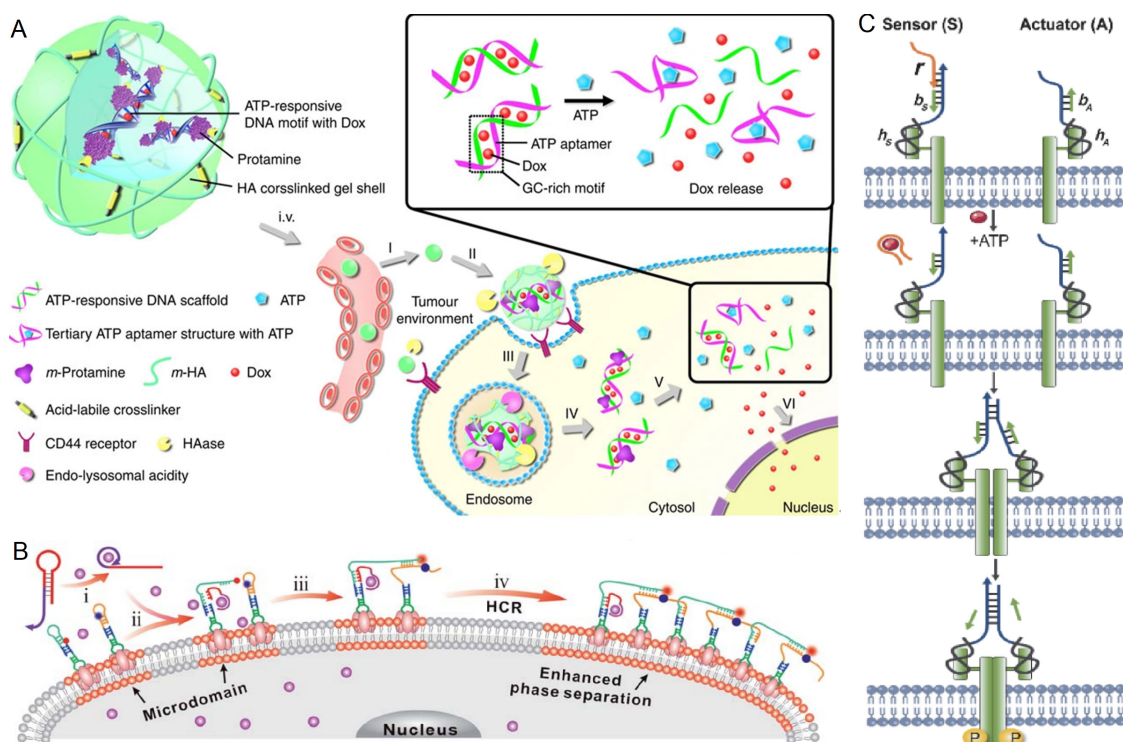


Figure 7. Schematic design of (A) ATP-triggered Dox release system [88]. Reproduced with permission from Nat. Commun., published by Nature, 2014. (B) ATP-activated hybridization chain reaction on the cell membrane that enhances membrane phase separation [89]. (i) Initiator I opening by ATP; (ii) H1 opening by initiator I; (iii) H2 opening by H1; (iv) HCR reaction. Reproduced with permission from Chem. Sci., published by The Royal Society of Chemistry, 2022. (C) ATP-responsive D-CID [90]. Reproduced with permission from Angew. Chem. Int. Ed., published by Wiley, 2018.

In addition, ATP was also used as stimulus to regulate receptor clustering at the cell membrane for protein degradation and cellular behavior manipulation. Li et al. developed an ATP-activated DNA nanodevice to enhance membrane phase separation through the clustering of dynamic lipid rafts (Figure 7B) [89]. The designed DNA anchored on the cell membrane could be activated by the overexpressed ATP in the tumor microenvironment to form a long DNA duplex on the cell membrane, which improved membrane phase separation and inhibited cancer cell migration. This DNA nanodevice provides a novel approach to regulate membrane phase separation and thus control cell motility with DNA nanotechnologies, and the versatile programmability of DNA provides multiple possibilities for biomedical and therapeutic applications. Nie et al. demonstrate a nongenetic approach for small-molecule-controlled receptor activation and consequent cell behavior via DNA-mediated chemically induced dimerization (D-CID) (Figure 7C) [90]. After the DNA strand displacement in the presence of ATP, this DNA nanodevice could trigger the activation of c-Met via dimerization and induce c-Met signaling. Using various functional nucleic acids, D-CID could be used to manipulate the behaviors of multiple cell populations and facilitate the precise control of cellular systems for bioengineering and therapeutic applications.

Glutathione (GSH) displays a much higher expression level in multiple types of tumor cells; thus, it has been widely applied as the trigger for on-demand drug release and targeted cancer therapy. Using DNA origami technology, Ding et al. designed a multifunctional DNA nanodevice, which can encapsulate and efficiently deliver many molecules, including siRNA and chemotherapy drugs. Due to their precisely designed

structure and controlled payload release, the DNA-origami-based delivery carriers play important roles in controllable therapy [91].

3.2. Response to Biomacromolecules

3.2.1. Nucleic Acids

MicroRNAs (miRNAs), as a class of endogenous, single-stranded, small RNA molecules, are actively involved in and regulate many biological processes. Therefore, they affect gene expression and have potential applications as disease biomarkers [92]. The typical role of these small non-coding RNA is to affect messenger RNA (mRNA) through the recognition site of the 3' untranslated region (UTR), thus regulating its stability [93]. Some miRNAs and mRNAs have been reported to display abnormally high expression levels in cancer cells, which makes them one of the most highly effective and specific stimuli that trigger drug delivery systems. Ju and Liu et al. designed a DNA nanomachine (DNM) using miRNA-21 as a trigger and the siRNA produced through a cascade reaction can significantly inhibit VEGF mRNA and protein expression in cell and in vivo tumor growth (Figure 8A) [94]. The DNA/RNA hybrids (DR and D'R') are alternately arranged on the DNA scaffold, forming DNM, which was previously produced via rolling circle amplification (RCA). By hybridizing ssDNA (D or D') with specific RNA (R or R'), DR and D'R' are synthesized. Here, the 5' end of R is labeled with Cy3 (Cy3-R) for the in situ monitoring of cellular processes, and its 3' end has a complementary toehold with the 5' end of target miRNA. Intracellular target miRNA can recognize the toehold of R and hybridize with the first 22 nucleotides of R starting from the 3' end, correspondingly opening DR. The released part of D subsequently reacted with D', thus triggering a strand displacement reaction between DR and D'R', generating dsDNA (DD') on the DNA scaffold, and releasing siRNA (RR') and miRNA from DNM. The released miRNA continuously reacted with R, and triggered a strand displacement reaction between DR and D'R' with the generation of siRNA. In addition, a negatively charged DNM can form stable nanocomposites with cationic folate modified polyethylene imine (FPEI) to promote target-cell-specific delivery and help the endosomes of DNM escape into the cytoplasm.

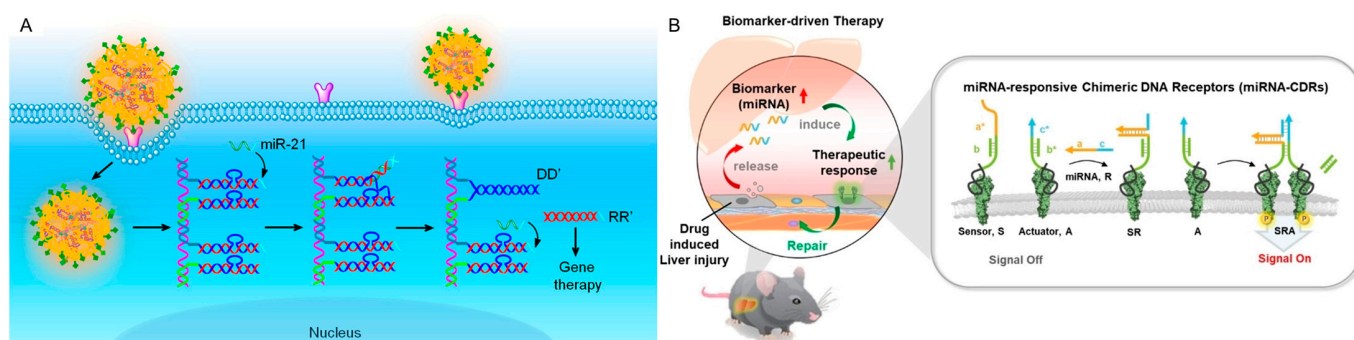


Figure 8. (A) Schematic illustration of intracellular siRNA cascade assembly with a microRNA-triggered DNM in living cells [94]. Reproduced with permission from ACS Nano, published by American Chemical Society, 2018. (B) miRNA-responsive DNA nanodevice for in situ repair and liver function restoration [95]. Reproduced with permission from Angew. Chem. Int. Ed., published by Wiley, 2023.

Using disease-associated extracellular miRNAs as input signals, Nie et al. presented a modular and programmable miRNA-responsive DNA nanodevice for biomarker-driven therapy (Figure 8B) [95]. The designed chimeric DNA receptor was grafted on a natural membrane receptor by virtue of aptamer anchoring, and the extracellular miRNA could trigger complementary-mediated strand displacement reaction to autonomously induce dimerization-mediated receptor activation. The in vivo experimental results demonstrated

the promoted MET signaling of hepatocytes and in situ repair and liver function restoration of this DNA nanodevice.

3.2.2. Proteins

Protein-responsive DNA nanostructures play a significant role in tumor therapy by providing targeted and controlled drug delivery systems [96] or activating therapeutic operation [97]. These nanostructures are designed to respond to specific proteins that are overexpressed in tumor cells for the selective delivery of therapeutic agents to the tumor site or enhance the cell apoptosis.

The design of oligonucleotide-based synthetic switches can be used to reprogram ligand specificity of growth factor receptors. The aptamer domain of the bispecific aptamer can be tailored for specific external cues. Sando et al. reported the DNA aptamer-mediated Reprogramming of the Interaction Partner of Receptor tyrosine kinases (DRIPaR). DRIPaR is based on bispecific DNA aptamers, which consist of an aptamer sequence that binds to the target RTK and another aptamer sequence that binds to a given cue in the extracellular space. The binding of growth factors induces dimerization of RTK and subsequent phosphorylation of intracellular domains is a key step in triggering the intracellular signaling cascade. Two bifunctional aptamers will form a ternary complex with one PDGF homodimer to induce Met activation. This approach could potentially be applied to design a new class of chemical tools that can control the activity of natural cells and represent smart and safe re-generative medicine [98]. By using DNA origami, Ding et al. built an autonomous DNA robot capable of transporting payloads and presenting them specifically in tumors. The nucleolin-targeting aptamer as targeting domains and molecular triggers for DNA nanorobots enables DNA nanorobots to perform precise drug delivery. In the presence of nucleolin, the aptamer at both ends of the tube nanocarrier bonded with nucleolin, breaking the binding of two sides and opening the tube into DNA sheet to expose the encapsulated thrombin [96].

Using the recognition of aptamers to cell membrane proteins, Yang et al. proposed a two-step self-assembling strategy based on the selective Watson–Crick base pairing properties of oligonucleotides (Figure 9A) [97]. This pretargeting–postassembly approach multivalently tethers receptor-prebound antibodies to albumin at the cell surface, allowing sequential actions of receptor binding and clustering to induce cell death.

Vascular endothelial growth factor (VEGF) is a signaling protein secreted by cells, used to promote the growth of new blood vessels. Due to its relatively higher expression around cancer cells compared to normal cells, it has been widely studied as a cancer biomarker and therapeutic target for cancer treatment plans. Liu et al. selected subcutaneous Raji lymphoma as a tumor model to develop a selective receptor aggregation (SMARC) strategy, which selectively aggregated CD20 on cell membrane via VEGF secretion (Figure 9B) [99]. Considering the cell membrane receptor CD20 is not only expressed by cancer cells, but also normal cells, merely CD20 specificity is not enough to achieve therapeutic precision. Therefore, incorporating the capability of cell selectivity to responsive DNA nanostructure is very important. By hybridizing DNA strands S, H, and H₂, DNA nanostrings with extended configurations (EDNS) were synthesized. In order to anchor EDNS to Raji cell membrane, it was hybridized with CD20 antibody-conjugated DNA strands (H₃-CD20) to obtain CD20 antibody-conjugated DNA nanochains (EDNS-CD20). The hairpin fragment with 27 bp and many repetitive units S/H provides sufficient length difference between the EDNS and CDNS (contracted DNA nanostring) configurations for DNA nanostrings (DNS). After intravenous injection, EDNS-CD20 recognized the CD20 receptor and bound to the Raji cell membrane. VEGF, as a cytokine selectively secreted by cancer cells, was chosen to distinguish cancer cells from normal cells. The designed VEGF amplifier consisted of cyclic reactions between double-stranded DNA strand IS-Apt_{VEGF} and DNA strand H₁, IS, and DNA nanochains. IS-Apt_{VEGF} recognized and bound to VEGF secreted by Raji cells, which released DNA strand IS. IS then hybridized with DNA strand H₁ to unfold its hairpin structure. The obtained IS-H₁ double stranded body served as a trigger for

the configuration change of DNA nanostrings: IS-H1 hybridized with EDNS through a toehold in H2 and generated the DNA nanostrings in transient state (TDNS). The strand displacement reaction between IS-H1 and H2 continues, which pulled H2 away from the DNA nanostring, thus restoring the hairpin structure of H and transformed the DNA nanostring into a contractile configuration (CDNS). This process also regenerated IS, which continuously hybridized with H1 for multiple reaction cycles, amplified the VEGF effect and led to the effective contraction of the DNA nanostring on cell membrane with CD20 clustering. The CD20 receptor aggregation then resulted in calcium influx and cell apoptosis. Binding to IS-Apt_{VEGF} can also inactivate VEGF, thereby blocking the activation of the VEGF receptor (VEGFR) and further facilitating tumor treatment.

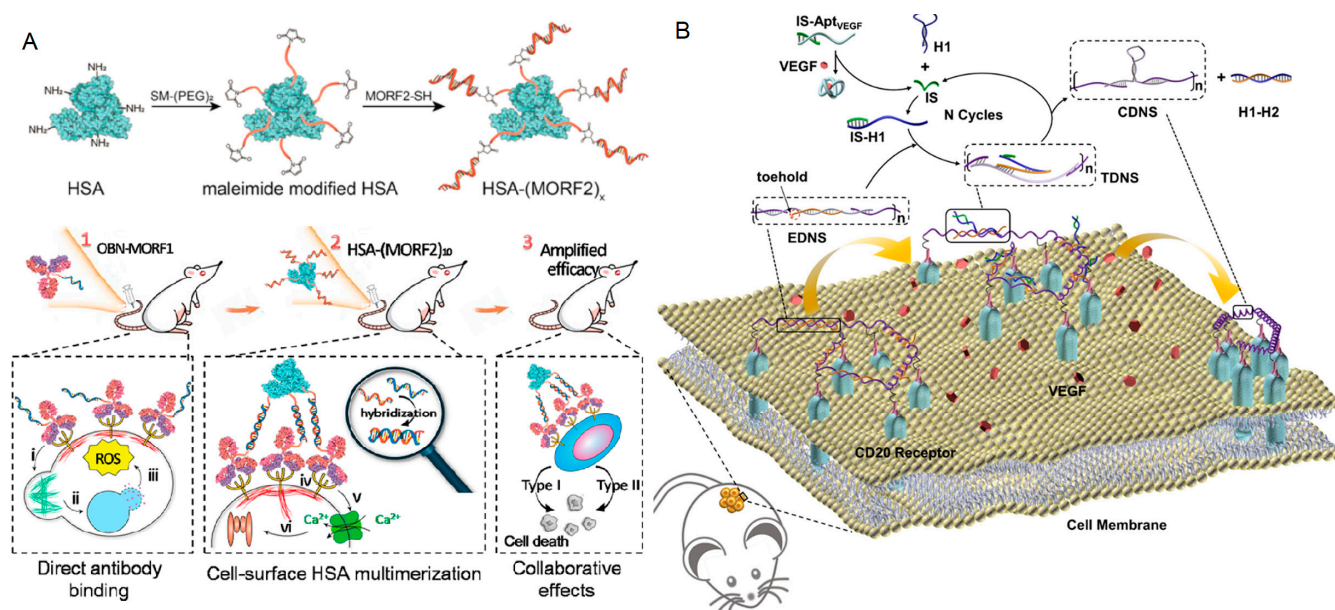


Figure 9. (A) Illustration of synthesis of conjugates and the pretargeting–postassembly approach that assembles OBN antibodies at cell surface [97]. (i) Actin remodeling, (ii) lysosome disruption, (iii) ROS production, (iv) receptor crosslinking, (v) calcium influx, (vi) caspase activation. Reproduced with permission from ACS Nano, published by American Chemical Society, 2019. (B) Vascular endothelial growth factor (VEGF) secreted by Raji cells regulated CD20 receptors aggregation on cell membrane [99]. Reproduced with permission from J. Am. Chem. Soc., published by American Chemical Society, 2023.

3.3. Response to Light Irradiation

Light is an exogenous, noninvasive stimulus that has superior spatiotemporal controllability and accuracy, and the rapid development of optical techniques provides operational convenience and decreases costs. Therefore, it has been widely used in controlled drug delivery and corresponding therapy.

Liu et al. designed a DNA copolymer nanocage that self-assembled on the cell membrane to encapsulate individual T cells and could be peeled off from cell membrane upon UV irradiation (Figure 10A) [100]. The photo-responsive DNA nanocage contained a self-quenched IFN- γ aptamer, which responded to IFN- γ secretion and restored fluorescence to indicate the activity of individual T cells. The wrapping of DNA nanocage confined the diffusion of secreted IFN- γ and eliminated interference from nearby cell secretion. Afterwards, active T cells were collected via flow cytometry and cell sorting, and subsequently exposed to 5 min of ultraviolet radiation to release nanocages from the cell membrane. Jurkat cells and CD19 CAR-T cells with higher activity were successfully selected with enhanced downstream cell activation and cancer cell killing capability. Yang et al. proposed a nongenetic approach for logic actuation of endogenous receptor assembly and corre-

sponding modulation of signal transduction via aptamer recognition and receptor assembly (Figure 10B) [101]. Under the activation of nucleic acid molecules and/or light irradiation, DNA logic assembly brings c-Met and CD71 into close proximity, which interfered with the ligand–receptor interactions of c-Met. This programmable design has been successfully exemplified for modulating cellular signal transduction and provides a convenient tool for biomedical applications.

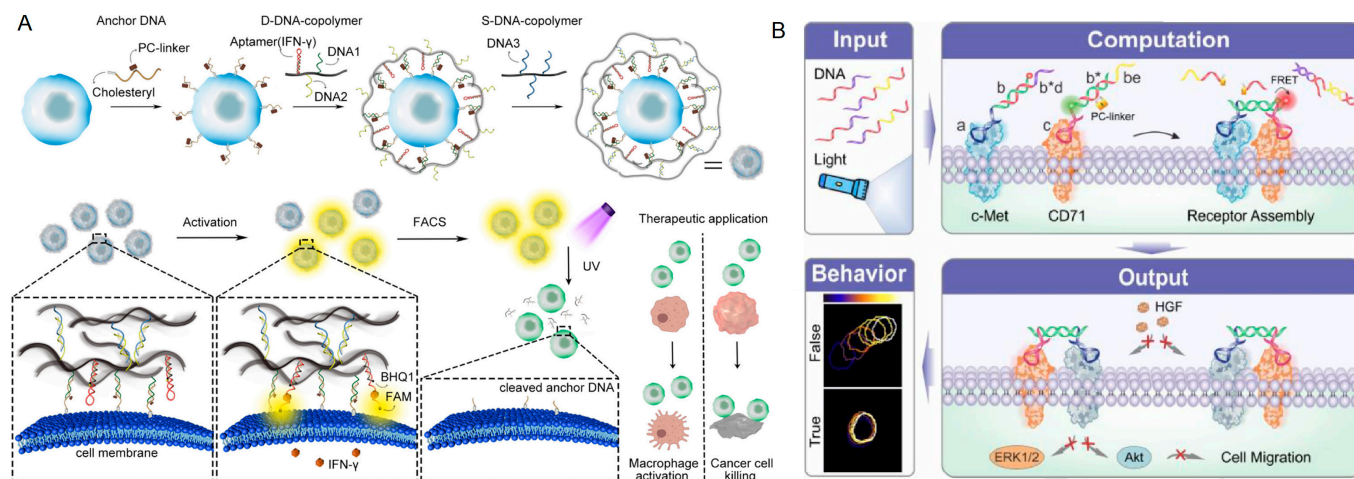


Figure 10. (A) Ultraviolet-light-induced DNA copolymer nanocage disassembly and corresponding cell activity sorting [100]. Reproduced with permission from Anal. Chem., published by American Chemical Society, 2022. (B) Logical aptamer-controlled receptor assembly for modulating cellular signal transduction [101]. Reproduced with permission from Angew. Chem. Int. Ed., published by Wiley, 2019.

Considering the poor tissue penetration and phototoxicity of UV or visible light, near-infrared (NIR) light is more appropriate for biomedical applications. Ju and Liu et al. designed a DNA–azobenzene nanopump for rapid and efficient drug release through combining DNA nanostructures with upconversion nanoparticles (UCNPs), which converted NIR light to UV and visible light (Figure 11A) [102]. DNA hybrids that assembled on UCNPs continuously switched configuration upon NIR irradiation, which act as the pump-type switcher. The anticancer drug doxorubicin (DOX) can selectively insert into GC base pairs of DNA for efficient loading. The continuous rotation–inversion movement of the phenyl moiety of azo in the hybridization zone of DNA backbones (DNA strands LAAzo, LCAzo with three azo moieties per DNA strand) resulted in the switching of DNA hybridization and dehybridization status, which facilitated DOX release. Moreover, HIV-1 TAT is a nuclear localization peptide that was conjugated to the DNA–azo nanopump for nuclear targeting. Itamar Willner’s group introduced different orthonitrobenzyl phosphate protective nucleic acids as functional units to induce liposome cell fusion processes (Figure 11B). Liposome L1 was loaded with upconversion nanoparticles (UCNP) and doxorubicin (DOX), which emitted light at 365 nm under near-infrared radiation (980 nm). HeLa cells were functionalized with a cholesterol-labelled DNA strand, and liposome was modified with complimentary DNA strand. The hybridization of the HeLa DNA strand and liposome DNA strand was prevented by a photo sealing strand, which was cleaved upon NIR irritation and facilitated liposome–cell fusion, thus realizing the space–time control of membrane fusion [103].

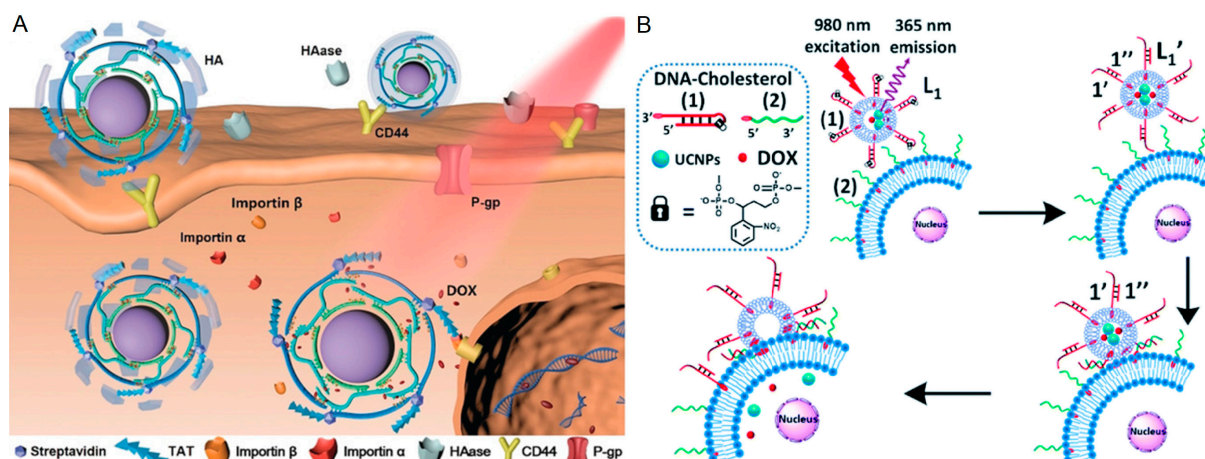


Figure 11. Near-infrared-light-induced (A) DNA Azobenzene Nanopump [102]. Reproduced with permission from *Angew. Chem. Int. Ed.*, published by Wiley, 2019. (B) Liposome cell membrane fusion system [103]. After the cleavage of hairpin (1), the liposome linked to cells by nucleic acid (2), resulting in the fusion and the release of DOX. Reproduced with permission from *Chem. Sci.*, published by The Royal Society of Chemistry, 2020.

Using the photothermal effect of gold nanoparticles, Liu et al. reported a design principle for stabilizing upconversion nanoparticles based on the coupling of small-sized Au nanoparticles (≈ 2 nm) and hairpin DNA (hpDNA) conjugation. The coupling of gold to up-converting nanoparticles modulates luminescence in the near-infrared region (≈ 800 nm). HpDNA strands allow for efficient drug loading through the double helix, which turned into single strands and released the loads under the high temperature generated from the gold nanoparticles under NIR light. The ideal platform for the constructed upconverted Au nanoconjugates enables simultaneous deep tissue imaging and site-specific anticancer drug administration [104].

3.4. Dual-Responsive DNA Nanostructures

Considering the complexity of physiological environment and the dynamical change of biomarker expression levels, DNA nanostructure activation only relied on a single stimulus that would bring in “off-target” toxicity and side effect. Therefore, “dual responsive” DNA nanostructure has been developed in the last few years to improve targeting precision and minimize the toxicity to circumjacent normal cells and tissues.

Furthermore, dual-responsive DNA nanostructures can also perform cell-subtype-specific recognition and precise drug delivery through multi-step DNA reactions. Ju’s group designed a ‘dual lock-and-key’ strategy to achieve controllable and accurate siRNA delivery through successive responses to two receptors on the cell membrane of CEM cells (Figure 12A) [105]. The triangular rung units (TRUs) with two overhangs at each end were synthesized as building blocks for ONV. Then, siRNAs were hybridized with the overhangs of TRU. The siRNA–TRUs were subsequently assembled with a long continuous DNA backbone strand produced by rolling circle amplification (RCA) to form siRNA–ONV. The hairpin structure of the DNA primer had an auto-cleavable position, which could be autocatalytically cleaved by the Zn^{2+} -dependent DNAzyme contained in *sgc4f* aptamer to form a DNA single strand. The cleaved single-strand DNA primer continuously hybridized with *sgc8c* aptamer to open its hairpin structure, acting as a smart key to be activated on-site by reacting sequentially with double locks *sgc4f* and *sgc8c*. The “dual locks and key” strategy resulted in efficient siRNA delivery and gene silencing.

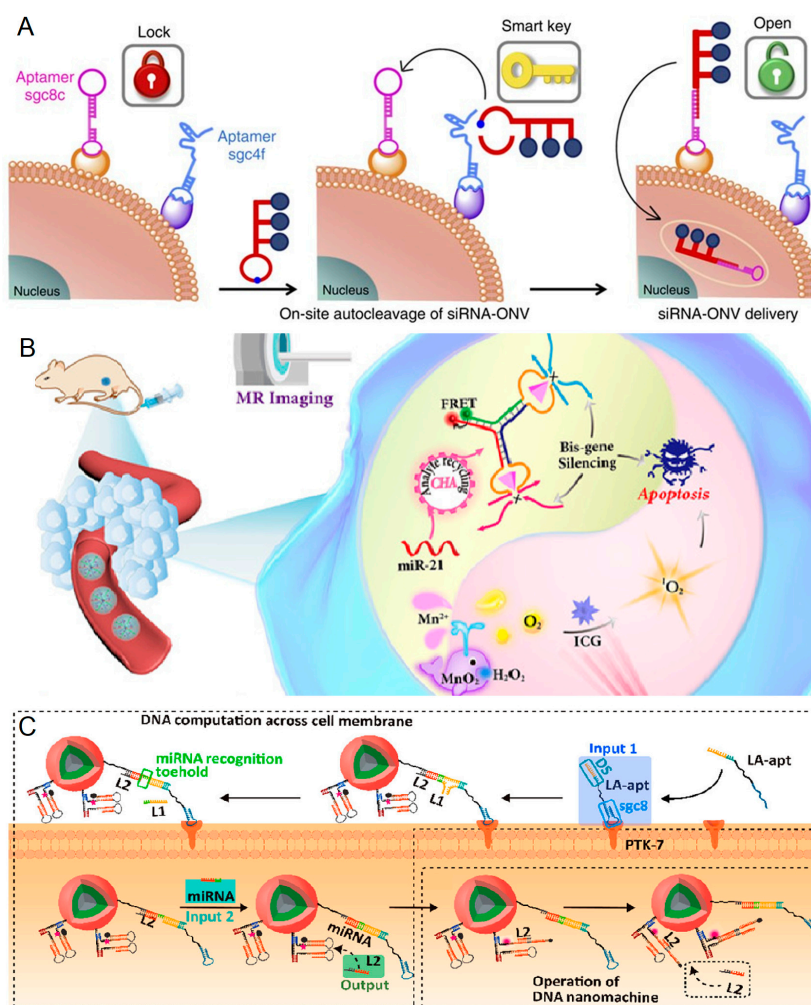


Figure 12. (A) Continuous activation of double-locked sgc4f and sgc8c with automatic DNA cutting hairpin structure system [105]. Reproduced with permission from Nat. Commun., published by Nature, 2016. (B) Endogenous miRNA-21 catalyzed DNA enzyme-mediated mRNA silencing system [106]. Reproduced with permission from Angew. Chem. Int. Ed., published by Wiley, 2020. (C) MiRNA-21/PTK7 dual-response DNA nanosystem [107]. Reproduced with permission from J. Am. Chem. Soc., published by American Chemical Society, 2021.

MiRNA-21 and H_2O_2 , which were highly expressed in the cancer cell, were also selected as stimuli to activate DNA nanomachine. Wang's group designed a biocompatible nanocapsule composed of DNAzyme prodrug and MnO_2 with tumor-specific recognition/activation characteristics (Figure 12B). The DNA probe in this nanocapsule is labeled with ICG, a near-infrared anthocyanin dye that can effectively convert near-infrared light to temperature increase and reactive oxygen species (ROS) generation, efficiently internalized DNA nanocomposite into the cytoplasm of tumor cells. PLGA (poly (D, L-lactide glycolic acid) scaffold was also decomposed through the photothermal effect of ICG, which exposed MnO_2 to endogenous H_2O_2 , and effectively generated Mn^{2+} ion for gene silencing [106].

Taking advantage of their aberrant expression at cancer cells, miRNAs have been applied as trigger to activate DNA nanomachine for precise therapy. However, the extensive distribution of miRNAs in the microenvironment of tumors and systemic circulation might induce nonspecific activation before the nanoprobe entering tumor cells, which impairs therapeutic efficiency and causes side effects on normal tissues and organs. To solve this problem, miRNA and cell membrane receptor were used as dual stimuli to activate DNA nanomachine. Ju and Liu's group designed a miRNA/PTK7-responsive DNA nanomachine (Figure 12C) [107], which achieved high-precision treatment only for cancer cells

in the complex solid tumor microenvironment. The DNA nanomachine is composed of multishell-structured upconversion nanoparticles (multishell UCNPs) and DNA frames L012 (assembled by DNA strands L0, L1, L2) and H012 (assembled by DNA strands H0, H1, H2). LA-apt is a DNA strand containing an 18bp DNA fragment (DS) and *sgc8* aptamer, which acted as input 1 for DNA calculation. DS captures DNA nanomachines and reacts with them, while protein tyrosine kinase-7 (PTK7) overexpressed on cancer cell membranes acts as the first responsive signal to target *sgc8*. Select intracellular miRNA-21 acted as input 2 for DNA calculation. L012 contained a DS hybridization zone and a miRNA-21 hybridization zone for “AND” gate operation. To perform an “AND” logic gate across the cell membrane, DS was hybridized with L012 via toehold T1, which releases L1 and exposes toehold T2 for miRNA recognition. Moreover, it also anchors the DNA nanomachine to the cancer cell membrane and facilitated subsequent endocytosis process. Self-quenched H1 is prepared by labeling photosensitizer Rose Bengal (RB) and its corresponding quencher BHQ in proximate positions. To operate the DNA nanomachine, L2 hybridized with H1 and opened its hairpin structure to activate RB with reactive oxygen species (ROS) generation under the green emission of multishell UCNPs upon 808 nm light irradiation. The unfolded H1 subsequently hybridized with adjacent H2, which set L2 free to react with the next H012 for continuous RB activation. This results in efficient photo-dynamic therapy (PDT).

4. Conclusions and Perspectives

Due to their structural programmability and good biocompatibility, DNA nanostructures have been widely applied in bioanalysis and therapy. External stimuli-responsive DNA strands such as metal-ion-bridged duplexes, i-motifs, triplex nucleic acids, G-quadruplexes, and programmed double-stranded hybrids of oligonucleotides have been widely explored and incorporated into DNA nanostructures for bioanalysis and cancer therapy with prospective outcomes. In this review, we outlined the advancements in stimuli-responsive DNA nanostructures construction and their applications in biomolecules sensing and cancer therapy.

Despite the remarkable progress in the field of stimuli-responsive DNA nanostructures for bioanalysis and therapy, the *in vivo* stability of DNA structures would be a big challenge for their further application. Phosphorothioate modification, covalent linkage between basic groups [108], and establishing a double-stranded rigid structure effectively enhanced the stability of DNA strands [109]. *Ex vivo* applications of DNA nanostructures for the detection of EVs or CTCs are more achievable in real use. In addition, there are still several challenges to be considered: (i) DNA nanostructures need specific ionic strength to maintain their morphology, which makes them less stable under physiological conditions and fragile to nucleases *in vivo*. Modification on the backbone or bases would enhance their stability. (ii) The negative charge of DNA nanostructure may bring difficulty for the endocytosis process, and generating a rigid structure would contribute to the effective intracellular delivery of the DNA nanostructure. (iii) Most currently reported DNA nanostructures demonstrated good target specificity, which is not enough for complicated *in vivo* conditions. Cell selectivity beyond target specificity with the selective discrimination between the normal cell and cancer cell that express the same target is also very important for *in vivo* application. With progress in the above-mentioned field, we truly believe that stimuli-responsive DNA nanostructures would establish an appealing toolbox for precise bioanalysis and personalized cancer therapy.

Funding: This research was funded by the National Natural Science Foundation of China (22022405, 22374073, 21974064), State Key Laboratory of Analytical Chemistry for Life Science (5431ZZXM2204, 5431ZZXM2307).

Data Availability Statement: Not available.

Conflicts of Interest: The authors declare no conflict of interest.

Abbreviations

| | |
|---------|--|
| miRNA | microRNA |
| HCR | Hybridization chain reaction |
| CHA | Catalytic hairpin assembly |
| RCA | Rolling circle amplification |
| MCP | miRNA capture probe |
| EVs | Extracellular vesicles |
| MB | Methylene blue |
| Exo III | Exonuclease III |
| SNAs | Spherical nucleic acids |
| CTCs | Circulating tumor cells |
| AP | aptamer |
| FluoELs | Fluorophores-encoded error-corrected labels |
| MSNs | Mesoporous silica nanoparticles |
| PC | Photo-cleavable |
| DQAsome | Dequalinium-based Liposome-like vesicle |
| UCNPs | Upconversion nanoparticles |
| NIR | Near-infra-red |
| AHA | Autocatalytic hybridization assembly |
| Dox | Doxorubicin |
| iDNS | Interlocked DNA nano-spring |
| ATP | 5'-adenosine triphosphate |
| HA | Hyaluronic acid |
| D-CID | DNA-mediated chemically induced dimerization |
| GSH | Glutathione |
| mRNA | messenger RNA |
| UTR | 3' untranslated region |
| DR/D'R' | DNA/RNA hybrids |
| SMARC | Selective receptor aggregation |
| PLGA | Poly (D, L-lactide glycolic acid |
| ROS | Reactive oxygen species |
| PDT | Photo-dynamic therapy |

References

1. Mo, L.; Liang, D.; Qin, R.; Mo, M.; Yang, C.; Lin, W. Three-Dimensional CHA-HCR System Using DNA Nanospheres for Sensitive and Rapid Imaging of miRNA in Live Cells and Tissues. *Anal. Chem.* **2023**, *95*, 11777–11784. [[CrossRef](#)] [[PubMed](#)]
2. Ai, L.; Zuo, Q.; Li, Y.; Wu, S.; Sima, Y.; Zhang, Y.; Xie, S.; Zhao, Z.; Tan, W. Programming Affinity for Precise Tumor Recognition with Allosteric Nanosensing-Circles. *ACS Nano* **2023**, *17*, 13430–13440. [[CrossRef](#)] [[PubMed](#)]
3. Zhi, S.; Zhang, X.; Zhang, J.; Wang, X.Y.; Bi, S. Functional Nucleic Acids-Engineered Bio-Barcode Nanoplatforams for Targeted Synergistic Therapy of Multidrug-Resistant Cancer. *ACS Nano* **2023**, *17*, 13533–13544. [[CrossRef](#)]
4. Li, M.; Yang, G.; Zheng, Y.; Lv, J.; Zhou, W.; Zhang, H.; You, F.; Wu, C.; Yang, H.; Liu, Y. NIR/pH-triggered aptamer-functionalized DNA origami nanovehicle for imaging-guided chemo-phototherapy. *J. Nanobiotechnol.* **2023**, *21*, 186. [[CrossRef](#)]
5. Rothemund, P.W. Folding DNA to create nanoscale shapes and patterns. *Nature* **2006**, *440*, 297–302. [[CrossRef](#)]
6. Ma, S.; Ren, Q.; Jiang, L.; Liu, Z.; Zhu, Y.; Zhu, J.; Zhang, Y.; Zhang, M. A triple-aptamer tetrahedral DNA nanostructures based carbon-nanotube-array transistor biosensor for rapid virus detection. *Talanta* **2023**, *266*, 124973. [[CrossRef](#)]
7. Zhang, H.; Zheng, X.; Zhao, T.; Chen, Y.; Luo, Y.; Dong, Y.; Tang, H.; Jiang, J. Real-Time Monitoring of Exosomes Secretion from Single Cell Using Dual-Nanopore Biosensors. *ACS Sens.* **2023**, *8*, 2583–2590. [[CrossRef](#)]
8. Yang, C.; Shi, Y.; Zhang, Y.; He, J.; Li, M.; Huang, W.; Yuan, R.; Xu, W. Modular DNA Tetrahedron Nanomachine-Guided Dual-Responsive Hybridization Chain Reactions for Discernible Bivariate Assay and Cell Imaging. *Anal. Chem.* **2023**, *95*, 10337–10345. [[CrossRef](#)]
9. Xiao, M.; Zhu, M.; Yuan, R.; Yuan, Y. Dual-sensitized heterojunction PDA/ZnO@MoS(2) QDs combined with multilocus domino-like DNA cascade reaction for ultrasensitive photoelectrochemical biosensor. *Biosens. Bioelectron.* **2023**, *227*, 115151. [[CrossRef](#)]
10. Park, J.C.; Na, H.; Choi, S.; Jeon, H.; Nam, Y.S. Target-Catalyzed Self-Assembly of DNA-Streptavidin Nanogel for Enzyme-Free miRNA Assay. *Adv. Healthc. Mater.* **2023**, *12*, e2202076. [[CrossRef](#)]

11. Xue, Y.; Xie, H.; Wang, Y.; Feng, S.; Sun, J.; Huang, J.; Yang, X. Novel and sensitive electrochemical/fluorescent dual-mode biosensing platform based on the cascaded cyclic amplification of enzyme-free DDSA and functional nucleic acids. *Biosens. Bioelectron.* **2022**, *218*, 114762. [[CrossRef](#)] [[PubMed](#)]
12. Zhang, Y.; Chen, W.; Zhang, Y.; Zhang, X.; Liu, Y.; Ju, H. A Near-Infrared Photo-Switched MicroRNA Amplifier for Precise Photodynamic Therapy of Early-Stage Cancers. *Angew. Chem. Int. Ed.* **2020**, *59*, 21454–21459. [[CrossRef](#)] [[PubMed](#)]
13. Sun, H.; Wang, T.; Ma, W.; Huang, J.; Chen, B.; Cheng, H.; Duan, S.; He, X.; Jian, L.; Wang, K. A stable DNA Tetrahedra-AuNCs nanohybrid: On-site programmed disassembly for tumor imaging and combination therapy. *Biomaterials* **2022**, *288*, 121738. [[CrossRef](#)] [[PubMed](#)]
14. Yang, L.; Yu, S.; Yan, Y.; Bi, S.; Zhu, J.J. Upconversion Nanoparticle@Au Core-Satellite Assemblies for In Situ Amplified Imaging of MicroRNA in Living Cells and Combined Cancer Phototherapy. *Anal. Chem.* **2022**, *94*, 7075–7083. [[CrossRef](#)]
15. Chai, X.; Yi, D.; Sheng, C.; Zhao, J.; Li, L. A Remotely Controlled Nanosystem for Spatiotemporally Specific Gene Regulation and Combinational Tumor Therapy. *Angew. Chem. Int. Ed.* **2023**, *62*, e202217702. [[CrossRef](#)]
16. Baig, M.; Ma, J.; Gao, X.; Khan, M.A.; Ali, A.; Farid, A.; Zia, A.W.; Noreen, S.; Wu, H. Exploring the robustness of DNA nanotubes framework for anticancer theranostics toward the 2D/3D clusters of hypopharyngeal respiratory tumor cells. *Int. J. Biol. Macromol.* **2023**, *236*, 123988. [[CrossRef](#)]
17. Wang, J.; Li, J.; Chen, Y.; Liu, R.; Wu, Y.; Liu, J.; Yang, X.; Wang, K.; Huang, J. Size-Controllable and Self-Assembled DNA Nanosphere for Amplified MicroRNA Imaging through ATP-Fueled Cyclic Dissociation. *Nano Lett.* **2022**, *22*, 8216–8223. [[CrossRef](#)]
18. Yang, Y.; Cai, X.; Shi, M.; Zhang, X.; Pan, Y.; Zhang, Y.; Ju, H.; Cao, P. Biomimetic retractable DNA nanocarrier with sensitive responsivity for efficient drug delivery and enhanced photothermal therapy. *J. Nanobiotechnol.* **2023**, *21*, 46. [[CrossRef](#)]
19. Shen, Y.; Hu, M.; Li, W.; Chen, Y.; Xu, Y.; Sun, L.; Liu, D.; Chen, S.; Gu, Y.; Ma, Y.; et al. Delivery of DNA octahedra enhanced by focused ultrasound with microbubbles for glioma therapy. *J. Control. Release Off. J. Control. Release Soc.* **2022**, *350*, 158–174. [[CrossRef](#)]
20. Wang, D.; Liu, J.; Duan, J.; Ma, Y.; Gao, H.; Zhang, Z.; Liu, J.; Shi, J.; Zhang, K. Photocontrolled Spatiotemporal Delivery of DNA Immunomodulators for Enhancing Membrane-Targeted Tumor Photodynamic Immunotherapy. *ACS Appl. Mater. Interfaces* **2022**, *14*, 44183–44198. [[CrossRef](#)]
21. Chen, Y.; Ke, G.; Ma, Y.; Zhu, Z.; Liu, M.; Liu, Y.; Yan, H.; Yang, C.J. A Synthetic Light-Driven Substrate Channeling System for Precise Regulation of Enzyme Cascade Activity Based on DNA Origami. *J. Am. Chem. Soc.* **2018**, *140*, 8990–8996. [[CrossRef](#)] [[PubMed](#)]
22. Trinh, T.; Thompson, I.A.P.; Clark, F.; Remington, J.M.; Eisenstein, M.; Li, J.; Soh, H.T. A Photoresponsive Intramolecular Triplex Motif That Enables Rapid and Reversible Control of Aptamer Binding Activity. *ACS Nano* **2022**, *16*, 14549–14557. [[CrossRef](#)] [[PubMed](#)]
23. Asanuma, H.; Liang, X.; Nishioka, H.; Matsunaga, D.; Liu, M.; Komiyama, M. Synthesis of Azobenzene-Tethered DNA for Reversible Photo-Regulation of DNA Functions: Hybridization and Transcription. *Nat. Protoc.* **2007**, *2*, 203–212. [[CrossRef](#)]
24. Ebrahimi, S.; Akhlaghi, Y.; Kompany-Zareh, M.; Rinnan, A. Nucleic acid based fluorescent nanothermometers. *ACS Nano* **2014**, *8*, 10372–10382. [[CrossRef](#)]
25. Mariottini, D.; Idili, A.; Ercolani, G.; Ricci, F. Thermo-Programmed Synthetic DNA-Based Receptors. *ACS Nano* **2023**, *17*, 1998–2006. [[CrossRef](#)]
26. Du, X.; He, P.-P.; Wang, C.; Wang, X.; Mu, Y.; Guo, W. Fast Transport and Transformation of Biomacromolecular Substances via Thermo-Stimulated Active “Inhalation-Exhalation” Cycles of Hierarchically Structured Smart pNIPAM-DNA Hydrogels. *Adv. Mater.* **2023**, *35*, e2206302. [[CrossRef](#)]
27. Maret, G.; Schickfus, M.v.; Mayer, A.; Dransfeld, K. Orientation of Nucleic Acids in High Magnetic Fields. *Phys. Rev. Lett.* **1975**, *35*, 397–400. [[CrossRef](#)]
28. Wang, Y.; Yang, Y.; Cao, X.; Liu, Z.; Chen, B.; Du, Q.; Lu, X. Simple and Ultrasensitive Detection of Glioma-Related ctDNAs in Mice Serum by SERS-Based Catalytic Hairpin Assembly Signal Amplification Coupled with Magnetic Aggregation. *Int. J. Nanomed.* **2023**, *18*, 3211–3230. [[CrossRef](#)]
29. Hallaj, R.; Ghafary, Z.; Kamal Mohammed, O.; Shakeri, R. Induced ultrasensitive electrochemical biosensor for target MDA-MB-231 cell cytoplasmic protein detection based on RNA-cleavage DNAzyme catalytic reaction. *Biosens. Bioelectron.* **2023**, *227*, 115168. [[CrossRef](#)]
30. Serrano-Chacón, I.; Mir, B.; Cupellini, L.; Colizzi, F.; Orozco, M.; Escaja, N.; González, C. pH-Dependent Capping Interactions Induce Large-Scale Structural Transitions in i-Motifs. *J. Am. Chem. Soc.* **2023**, *145*, 3696–3705. [[CrossRef](#)]
31. Luo, H.; Wang, Z.; Mo, Q.; Yang, J.; Yang, F.; Tang, Y.; Liu, J.; Li, X. Framework Nucleic Acid-Based Multifunctional Tumor Theranostic Nanosystem for miRNA Fluorescence Imaging and Chemo/Gene Therapy. *ACS Appl. Mater. Interfaces* **2023**, *15*, 33223–33238. [[CrossRef](#)] [[PubMed](#)]
32. Deng, J.; Walther, A. ATP-Responsive and ATP-Fueled Self-Assembling Systems and Materials. *Adv. Mater.* **2020**, *32*, e2002629. [[CrossRef](#)] [[PubMed](#)]
33. Kim, N.; Kim, E.; Kim, H.; Thomas, M.R.; Najer, A.; Stevens, M.M. Tumor-Targeting Cholesterol-Decorated DNA Nanoflowers for Intracellular Ratiometric Aptasensing. *Adv. Mater.* **2021**, *33*, e2007738. [[CrossRef](#)] [[PubMed](#)]

34. Yin, Q.; Zhao, D.; Chang, Y.; Liu, B.; Liu, Y.; Liu, M. Functional DNA Superstructures Exhibit Positive Homotropic Allostery in Ligand Binding. *Angew. Chem. Int. Ed.* **2023**, *135*, e202303838. [[CrossRef](#)]
35. Ren, Q.; Jiang, L.; Ma, S.; Li, T.; Zhu, Y.; Qiu, R.; Xing, Y.; Yin, F.; Li, Z.; Ye, X.; et al. Multi-Body Biomarker Entrapment System: An All-Encompassing Tool for Ultrasensitive Disease Diagnosis and Epidemic Screening. *Adv. Mater.* **2023**, e2304119. [[CrossRef](#)]
36. Meng, R.; Zhang, X.; Liu, J.; Zhou, Y.; Zhang, P.; Chai, Y.; Yuan, R. Dual-layer 3D DNA nanostructure: The next generation of ultrafast DNA nanomachine for microRNA sensing and intracellular imaging. *Biosens. Bioelectron.* **2023**, *237*, 115517. [[CrossRef](#)]
37. Yu, L.; Peng, Y.; Sheng, M.; Wang, Q.; Huang, J.; Yang, X. Sensitive and Amplification-Free Electrochemiluminescence Biosensor for HPV-16 Detection Based on CRISPR/Cas12a and DNA Tetrahedron Nanostructures. *ACS Sens.* **2023**, *8*, 2852–2858. [[CrossRef](#)]
38. Rossi-Gendron, C.; El Fakih, F.; Bourdon, L.; Nakazawa, K.; Finkel, J.; Triomphe, N.; Chocron, L.; Endo, M.; Sugiyama, H.; Bellot, G.; et al. Isothermal self-assembly of multicomponent and evolutive DNA nanostructures. *Nat. Nanotechnol.* **2023**. [[CrossRef](#)]
39. Jin, Y.; Huang, Z.; Xu, B.; Chen, J. Localization of multiple DNAzymes as a branchedzyme-powered nanodevice for the immunoassay of tumor biomarkers. *Anal. Chim. Acta* **2023**, *1274*, 341580. [[CrossRef](#)]
40. Xing, Y.; Dorey, A.; Howorka, S. Multi-Stimuli-Responsive and Mechano-Actuated Biomimetic Membrane Nanopores Self-Assembled from DNA. *Adv. Mater.* **2023**, *35*, e2300589. [[CrossRef](#)]
41. Xue, Y.Q.; Liao, N.; Li, Y.; Liang, W.B.; Yang, X.; Zhong, X.; Zhuo, Y. Ordered heterogeneity in dual-ligand MOF to enable high electrochemiluminescence efficiency for bioassay with DNA triangular prism as signal switch. *Biosens. Bioelectron.* **2022**, *217*, 114713. [[CrossRef](#)] [[PubMed](#)]
42. Zhou, C.; Chuai, Y.; Lin, C.; Wang, D.; Wang, Q.; Zou, H. A dual fragment triggered DNA ladder nanostructure based on logic gate and dispersion-to-localization catalytic hairpin assembly for efficient fluorescence assay of SARS-CoV-2 and H1N1. *Anal. Chim. Acta* **2023**, *1275*, 341590. [[CrossRef](#)]
43. Deng, W.; Xu, J.Y.; Peng, H.; Huang, C.Z.; Le, X.C.; Zhang, H. DNAzyme motor systems and logic gates facilitated by toehold exchange translators. *Biosens. Bioelectron.* **2022**, *217*, 114704. [[CrossRef](#)] [[PubMed](#)]
44. Zhou, X.M.; Zhuo, Y.; Yuan, R.; Chai, Y.Q. Target-mediated self-assembly of DNA networks for sensitive detection and intracellular imaging of APE1 in living cells. *Chem. Sci.* **2023**, *14*, 2318–2324. [[CrossRef](#)] [[PubMed](#)]
45. Shen, M.; Shi, J.; Chen, Z.; Zhang, S.; Zhang, Z. Self-assembly of DNA-hyperbranched aggregates catalyzed by a dual-targets recognition probe for miRNAs SERS detection in single cells. *Biosens. Bioelectron.* **2023**, *222*, 114997. [[CrossRef](#)]
46. Du, S.; Xie, B.; Gao, H.; Zhang, J.; Fu, H.; Liao, F.; Liao, Y. Self-Powered DNAzyme Walker Enables Dual-Mode Biosensor Construction for Electrochemiluminescence and Electrochemical Detection of MicroRNA. *Anal. Chem.* **2023**, *95*, 7006–7013. [[CrossRef](#)]
47. Garzon, R.; Calin, G.A.; Croce, C.M. MicroRNAs in Cancer. *Annu. Rev. Med.* **2009**, *60*, 167–179. [[CrossRef](#)]
48. Bartel, D.P. MicroRNAs: Target recognition and regulatory functions. *Cell* **2009**, *136*, 215–233. [[CrossRef](#)]
49. He, L.; Hannon, G.J. MicroRNAs: Small RNAs with a big role in gene regulation. *Nat. Rev. Genet.* **2004**, *5*, 522–531. [[CrossRef](#)]
50. Lu, J.; Getz, G.; Miska, E.A.; Alvarez-Saavedra, E.; Lamb, J.; Peck, D.; Sweet-Cordero, A.; Ebert, B.L.; Mak, R.H.; Ferrando, A.A.; et al. MicroRNA expression profiles classify human cancers. *Nature* **2005**, *435*, 834–838. [[CrossRef](#)]
51. Chen, X.; Ba, Y.; Ma, L.; Cai, X.; Yin, Y.; Wang, K.; Guo, J.; Zhang, Y.; Chen, J.; Guo, X.; et al. Characterization of microRNAs in serum: A novel class of biomarkers for diagnosis of cancer and other diseases. *Cell Res.* **2008**, *18*, 997–1006. [[CrossRef](#)]
52. Kim, T.H.; Lee, Y.; Lee, Y.S.; Gim, J.A.; Ko, E.; Yim, S.Y.; Jung, Y.K.; Kang, S.; Kim, M.Y.; Kim, H.; et al. Circulating miRNA is a useful diagnostic biomarker for nonalcoholic steatohepatitis in nonalcoholic fatty liver disease. *Sci. Rep.* **2021**, *11*, 14639. [[CrossRef](#)] [[PubMed](#)]
53. Wu, Q.; Li, L.; Jia, Y.; Xu, T.; Zhou, X. Advances in studies of circulating microRNAs: Origination, transportation, and distal target regulation. *J. Cell Commun. Signal.* **2022**, *17*, 445–455. [[CrossRef](#)] [[PubMed](#)]
54. Chapin, S.C.; Doyle, P.S. Ultrasensitive multiplexed microRNA quantification on encoded gel microparticles using rolling circle amplification. *Anal. Chem.* **2011**, *83*, 7179–7185. [[CrossRef](#)] [[PubMed](#)]
55. Wu, L.; Wang, Y.; He, R.; Zhang, Y.; He, Y.; Wang, C.; Lu, Z.; Liu, Y.; Ju, H. Fluorescence hydrogel array based on interfacial cation exchange amplification for highly sensitive microRNA detection. *Anal. Chim. Acta* **2019**, *1080*, 206–214. [[CrossRef](#)]
56. Guo, S.; Lin, W.N.; Hu, Y.; Sun, G.; Phan, D.T.; Chen, C.H. Ultrahigh-throughput droplet microfluidic device for single-cell miRNA detection with isothermal amplification. *Lab Chip* **2018**, *18*, 1914–1920. [[CrossRef](#)]
57. Li, L.; Lu, M.; Fan, Y.; Shui, L.; Xie, S.; Sheng, R.; Si, H.; Li, Q.; Wang, Y.; Tang, B. High-throughput and ultra-sensitive single-cell profiling of multiple microRNAs and identification of human cancer. *Chem. Commun.* **2019**, *55*, 10404–10407. [[CrossRef](#)]
58. Wang, Y.; Fang, Y.; Zhu, Y.; Bi, S.; Liu, Y.; Ju, H. Single cell multi-miRNAs quantification with hydrogel microbeads for liver cancer cell subtypes discrimination. *Chem. Sci.* **2022**, *13*, 2062–2070. [[CrossRef](#)]
59. Herrmann, I.K.; Wood, M.J.A.; Fuhrmann, G. Extracellular vesicles as a next-generation drug delivery platform. *Nat. Nanotechnol.* **2021**, *16*, 748–759. [[CrossRef](#)]
60. Buzas, E.I. The roles of extracellular vesicles in the immune system. *Nat. Rev. Immunol.* **2023**, *23*, 236–250. [[CrossRef](#)]
61. Nabet, B.Y.; Qiu, Y.; Shabason, J.E.; Wu, T.J.; Yoon, T.; Kim, B.C.; Benci, J.L.; DeMichele, A.M.; Tchou, J.; Marcotrigiano, J.; et al. Exosome RNA Unshielding Couples Stromal Activation to Pattern Recognition Receptor Signaling in Cancer. *Cell* **2017**, *170*, 352–366. [[CrossRef](#)]

62. Shen, W.; Guo, K.; Adkins, G.B.; Jiang, Q.; Liu, Y.; Sedano, S.; Duan, Y.; Yan, W.; Wang, S.E.; Bergersen, K.; et al. A Single Extracellular Vesicle (EV) Flow Cytometry Approach to Reveal EV Heterogeneity. *Angew. Chem. Int. Ed.* **2018**, *57*, 15675–15680. [[CrossRef](#)]
63. Wang, L.; Deng, Y.; Wei, J.; Huang, Y.; Wang, Z.; Li, G. Spherical nucleic acids-based cascade signal amplification for highly sensitive detection of exosomes. *Biosens. Bioelectron.* **2021**, *191*, 113465. [[CrossRef](#)] [[PubMed](#)]
64. Lin, D.; Shen, L.; Luo, M.; Zhang, K.; Li, J.; Yang, Q.; Zhu, F.; Zhou, D.; Zheng, S.; Chen, Y.; et al. Circulating tumor cells: Biology and clinical significance. *Signal Transduct. Target. Ther.* **2021**, *6*, 404. [[CrossRef](#)] [[PubMed](#)]
65. Eslami, S.Z.; Cortes-Hernandez, L.E.; Thomas, F.; Pantel, K.; Alix-Panabieres, C. Functional analysis of circulating tumour cells: The KEY to understand the biology of the metastatic cascade. *Br. J. Cancer* **2022**, *127*, 800–810. [[CrossRef](#)] [[PubMed](#)]
66. Peng, Y.; Pan, Y.; Han, Y.; Sun, Z.; Jalalah, M.; Al-Assiri, M.S.; Harraz, F.A.; Yang, J.; Li, G. Direct Analysis of Rare Circulating Tumor Cells in Whole Blood Based on Their Controlled Capture and Release on Electrode Surface. *Anal. Chem.* **2020**, *92*, 13478–13484. [[CrossRef](#)]
67. Song, Y.; Shi, Y.; Huang, M.; Wang, W.; Wang, Y.; Cheng, J.; Lei, Z.; Zhu, Z.; Yang, C. Bioinspired Engineering of a Multivalent Aptamer-Functionalized Nanointerface to Enhance the Capture and Release of Circulating Tumor Cells. *Angew. Chem. Int. Ed.* **2019**, *58*, 2236–2240. [[CrossRef](#)]
68. Zhang, J.; Lin, B.; Wu, L.; Huang, M.; Li, X.; Zhang, H.; Song, J.; Wang, W.; Zhao, G.; Song, Y.; et al. DNA Nanolithography Enables a Highly Ordered Recognition Interface in a Microfluidic Chip for the Efficient Capture and Release of Circulating Tumor Cells. *Angew. Chem. Int. Ed.* **2020**, *59*, 14115–14119. [[CrossRef](#)]
69. Wu, L.; Ding, H.; Qu, X.; Shi, X.; Yang, J.; Huang, M.; Zhang, J.; Zhang, H.; Song, J.; Zhu, L.; et al. Fluidic Multivalent Membrane Nanointerface Enables Synergetic Enrichment of Circulating Tumor Cells with High Efficiency and Viability. *J. Am. Chem. Soc.* **2020**, *142*, 4800–4806. [[CrossRef](#)]
70. Wei, J.; Wang, H.; Wu, Q.; Gong, X.; Ma, K.; Liu, X.; Wang, F. A Smart, Autocatalytic, DNAzyme Biocircuit for in Vivo, Amplified, MicroRNA Imaging. *Angew. Chem. Int. Ed.* **2020**, *59*, 5965–5971. [[CrossRef](#)]
71. He, S.; Yu, S.; Li, R.; Chen, Y.; Wang, Q.; He, Y.; Liu, X.; Wang, F. On-Site Non-enzymatic Orthogonal Activation of a Catalytic DNA Circuit for Self-Reinforced In Vivo MicroRNA Imaging. *Angew. Chem. Int. Ed.* **2022**, *61*, e202206529. [[CrossRef](#)] [[PubMed](#)]
72. Wang, H.; He, Y.; Wei, J.; Wang, H.; Ma, K.; Zhou, Y.; Liu, X.; Zhou, X.; Wang, F. Construction of an Autocatalytic Hybridization Assembly Circuit for Amplified In Vivo MicroRNA Imaging. *Angew. Chem. Int. Ed.* **2022**, *61*, e202115489. [[CrossRef](#)] [[PubMed](#)]
73. Dong, P.; Li, R.; He, S.; Zhang, Q.; Shang, J.; Jiang, Y.; Liu, X.; Wang, F. The compact integration of a cascaded HCR circuit for highly reliable cancer cell discrimination. *Chem. Sci.* **2023**, *14*, 2159–2167. [[CrossRef](#)] [[PubMed](#)]
74. Li, R.; Zhu, Y.; Gong, X.; Zhang, Y.; Hong, C.; Wan, Y.; Liu, X.; Wang, F. Self-Stacking Autocatalytic Molecular Circuit with Minimal Catalytic DNA Assembly. *J. Am. Chem. Soc.* **2023**, *145*, 2999–3007. [[CrossRef](#)] [[PubMed](#)]
75. Shang, J.; Yu, S.; Li, R.; He, Y.; Wang, Y.; Wang, F. Bioorthogonal Disassembly of Hierarchical DNAzyme Nanogel for High-Performance Intracellular microRNA Imaging. *Nano Lett.* **2023**, *23*, 1386–1394. [[CrossRef](#)]
76. Hong, S.; Zhang, X.; Lake, R.J.; Pawel, G.T.; Guo, Z.; Pei, R.; Lu, Y. A photo-regulated aptamer sensor for spatiotemporally controlled monitoring of ATP in the mitochondria of living cells. *Chem. Sci.* **2019**, *11*, 713–720. [[CrossRef](#)]
77. Wen, S.; Zhou, J.; Zheng, K.; Bednarkiewicz, A.; Liu, X.; Jin, D. Advances in highly doped upconversion nanoparticles. *Nat. Commun.* **2018**, *9*, 2415. [[CrossRef](#)]
78. Zhao, J.; Chu, H.; Zhao, Y.; Lu, Y.; Li, L. A NIR Light Gated DNA Nanodevice for Spatiotemporally Controlled Imaging of MicroRNA in Cells and Animals. *J. Am. Chem. Soc.* **2019**, *141*, 7056–7062. [[CrossRef](#)]
79. Wei, W.; Dai, W.; Yang, F.; Lu, H.; Zhang, K.; Xing, Y.; Meng, X.; Zhou, L.; Zhang, Y.; Yang, Q.; et al. Spatially Resolved, Error-Robust Multiplexed MicroRNA Profiling in Single Living Cells. *Angew. Chem. Int. Ed.* **2022**, *61*, e202116909. [[CrossRef](#)]
80. Zhang, Y.; Zhang, Y.; Zhang, X.; Li, Y.; He, Y.; Liu, Y.; Ju, H. A photo zipper locked DNA nanomachine with an internal standard for precise miRNA imaging in living cells. *Chem. Sci.* **2020**, *11*, 6289–6296. [[CrossRef](#)]
81. Li, Y.; Xie, Y.; Zhang, Y.; Zhao, H.; Ju, H.; Liu, Y. DNA nanomachine activation and Zn²⁺ imaging in living cells with single NIR irradiation. *Anal. Chim. Acta* **2022**, *1221*, 340149. [[CrossRef](#)] [[PubMed](#)]
82. He, C.; Lu, K.; Lin, W. Nanoscale metal-organic frameworks for real-time intracellular pH sensing in live cells. *J. Am. Chem. Soc.* **2014**, *136*, 12253–12256. [[CrossRef](#)] [[PubMed](#)]
83. Singh, A.K.; Nair, A.V.; Singh, N.D.P. Small Two-Photon Organic Fluorogenic Probes: Sensing and Bioimaging of Cancer Relevant Biomarkers. *Anal. Chem.* **2021**, *94*, 177–192. [[CrossRef](#)] [[PubMed](#)]
84. Zhang, P.; Ouyang, Y.; Sohn, Y.S.; Nechushtai, R.; Pikarsky, E.; Fan, C.; Willner, I. pH- and miRNA-Responsive DNA-Tetrahedra/Metal-Organic Framework Conjugates: Functional Sense-and-Treat Carriers. *ACS Nano* **2021**, *15*, 6645–6657. [[CrossRef](#)]
85. Liu, S.; Jiang, Q.; Zhao, X.; Zhao, R.; Wang, Y.; Wang, Y.; Liu, J.; Shang, Y.; Zhao, S.; Wu, T.; et al. A DNA nanodevice-based vaccine for cancer immunotherapy. *Nat. Mater.* **2021**, *20*, 421–430. [[CrossRef](#)]
86. Qian, R.C.; Zhou, Z.R.; Wu, Y.; Yang, Z.; Guo, W.; Li, D.W.; Lu, Y. Combination Cancer Treatment: Using Engineered DNAzyme Molecular Machines for Dynamic Inter- and Intracellular Regulation. *Angew. Chem. Int. Ed.* **2022**, *61*, e202210935. [[CrossRef](#)]
87. Zhang, K.; Ma, Y.; Wang, D.; Liu, J.; An, J.; Li, Y.; Ma, C.; Pei, Y.; Zhang, Z.; Liu, J.; et al. In Vivo Activation of T-Cell Proliferation by Regulating Cell Surface Receptor Clustering Using a pH-Driven Interlocked DNA Nano-Spring. *Nano Lett.* **2022**, *22*, 1937–1945. [[CrossRef](#)]
88. Mo, R.; Jiang, T.; DiSanto, R.; Tai, W.; Gu, Z. ATP-triggered anticancer drug delivery. *Nat. Commun.* **2014**, *5*, 3364. [[CrossRef](#)]

89. Su, Y.; Chen, X.; Wang, H.; Sun, L.; Xu, Y.; Li, D. Enhancing cell membrane phase separation for inhibiting cancer metastasis with a stimuli-responsive DNA nanodevice. *Chem. Sci.* **2022**, *13*, 6303–6308. [[CrossRef](#)]
90. Li, H.; Wang, M.; Shi, T.; Yang, S.; Zhang, J.; Wang, H.H.; Nie, Z. A DNA-Mediated Chemically Induced Dimerization (D-CID) Nanodevice for Nongenetic Receptor Engineering To Control Cell Behavior. *Angew. Chem. Int. Ed.* **2018**, *57*, 10226–10230. [[CrossRef](#)]
91. Wang, Z.; Song, L.; Liu, Q.; Tian, R.; Shang, Y.; Liu, F.; Liu, S.; Zhao, S.; Han, Z.; Sun, J.; et al. A Tubular DNA Nanodevice as a siRNA/Chemo-Drug Co-delivery Vehicle for Combined Cancer Therapy. *Angew. Chem. Int. Ed.* **2021**, *60*, 2594–2598. [[CrossRef](#)] [[PubMed](#)]
92. Yoon, A.J.; Wang, S.; Kutler, D.I.; Carvajal, R.D.; Philipone, E.; Wang, T.; Peters, S.M.; LaRoche, D.; Hernandez, B.Y.; McDowell, B.D.; et al. MicroRNA-based risk scoring system to identify early-stage oral squamous cell carcinoma patients at high-risk for cancer-specific mortality. *Head Neck* **2020**, *42*, 1699–1712. [[CrossRef](#)] [[PubMed](#)]
93. Lakhia, R.; Ramalingam, H.; Chang, C.M.; Cobo-Stark, P.; Biggers, L.; Flaten, A.; Alvarez, J.; Valencia, T.; Wallace, D.P.; Lee, E.C.; et al. PKD1 and PKD2 mRNA cis-inhibition drives polycystic kidney disease progression. *Nat. Commun.* **2022**, *13*, 4765. [[CrossRef](#)] [[PubMed](#)]
94. Ren, K.; Zhang, Y.; Zhang, X.; Liu, Y.; Yang, M.; Ju, H. In Situ siRNA Assembly in Living Cells for Gene Therapy with MicroRNA Triggered Cascade Reactions Templated by Nucleic Acids. *ACS Nano* **2018**, *12*, 10797–10806. [[CrossRef](#)]
95. He, F.; Wang, M.; Wang, J.; Wang, H.H.; Nie, Z. An Extracellular miRNA-Responsive Artificial Receptor via Dynamic DNA Nano-assembly for Biomarker-Driven Therapy. *Angew. Chem. Int. Ed.* **2023**, *135*, e202305227. [[CrossRef](#)]
96. Li, S.; Jiang, Q.; Liu, S.; Zhang, Y.; Tian, Y.; Song, C.; Wang, J.; Zou, Y.; Anderson, G.J.; Han, J.Y.; et al. A DNA nanorobot functions as a cancer therapeutic in response to a molecular trigger in vivo. *Nat. Biotechnol.* **2018**, *36*, 258–264. [[CrossRef](#)]
97. Li, L.; Wang, J.; Li, Y.; Radford, D.C.; Yang, J.; Kopeček, J. Broadening and Enhancing Functions of Antibodies by Self-Assembling Multimerization at Cell Surface. *ACS Nano* **2019**, *13*, 11422–11432. [[CrossRef](#)]
98. Ueki, R.; Atsuta, S.; Ueki, A.; Sando, S. Nongenetic Reprogramming of the Ligand Specificity of Growth Factor Receptors by Bispecific DNA Aptamers. *J. Am. Chem. Soc.* **2017**, *139*, 6554–6557. [[CrossRef](#)]
99. Bi, S.; Chen, W.; Fang, Y.; Wang, Y.; Zhang, Q.; Guo, H.; Ju, H.; Liu, Y. Cancer Cell-Selective Membrane Receptor Clustering Driven by VEGF Secretion for In Vivo Therapy. *J. Am. Chem. Soc.* **2023**, *145*, 5041–5052. [[CrossRef](#)]
100. Fang, Y.; Yan, Y.; Bi, S.; Wang, Y.; Chen, Y.; Xu, P.; Ju, H.; Liu, Y. Screening T-Cell Activity via a Photodetachable DNA-Copolymer Nanocage and Its Therapeutic Application. *Anal. Chem.* **2022**, *94*, 13205–13214. [[CrossRef](#)]
101. Chen, S.; Xu, Z.; Yang, W.; Lin, X.; Li, J.; Li, J.; Yang, H. Logic-Gate-Actuated DNA-Controlled Receptor Assembly for the Programmable Modulation of Cellular Signal Transduction. *Angew. Chem. Int. Ed.* **2019**, *58*, 18186–18190. [[CrossRef](#)]
102. Zhang, Y.; Zhang, Y.; Song, G.; He, Y.; Zhang, X.; Liu, Y.; Ju, H. A DNA-Azobenzene Nanopump Fueled by Upconversion Luminescence for Controllable Intracellular Drug Release. *Angew. Chem. Int. Ed.* **2019**, *58*, 18207–18211. [[CrossRef](#)]
103. Huang, F.; Duan, R.; Zhou, Z.; Vázquez-González, M.; Xia, F.; Willner, I. Near-infrared light-activated membrane fusion for cancer cell therapeutic applications. *Chem. Sci.* **2020**, *11*, 5592–5600. [[CrossRef](#)] [[PubMed](#)]
104. Han, S.; Samanta, A.; Xie, X.; Huang, L.; Peng, J.; Park, S.J.; Teh, D.B.L.; Choi, Y.; Chang, Y.T.; All, A.H.; et al. Gold and Hairpin DNA Functionalization of Upconversion Nanocrystals for Imaging and In Vivo Drug Delivery. *Adv. Mater.* **2017**, *29*, 1700244. [[CrossRef](#)] [[PubMed](#)]
105. Ren, K.; Liu, Y.; Wu, J.; Zhang, Y.; Zhu, J.; Yang, M.; Ju, H. A DNA dual lock-and-key strategy for cell-subtype-specific siRNA delivery. *Nat. Commun.* **2016**, *7*, 13580. [[CrossRef](#)] [[PubMed](#)]
106. Gong, X.; Li, R.; Wang, J.; Wei, J.; Ma, K.; Liu, X.; Wang, F. A Smart Theranostic Nanocapsule for Spatiotemporally Programmable Photo-Gene Therapy. *Angew. Chem. Int. Ed.* **2020**, *59*, 21648–21655. [[CrossRef](#)]
107. Zhang, Y.; Chen, W.; Fang, Y.; Zhang, X.; Liu, Y.; Ju, H. Activating a DNA Nanomachine via Computation across Cancer Cell Membranes for Precise Therapy of Solid Tumors. *J. Am. Chem. Soc.* **2021**, *143*, 15233–15242. [[CrossRef](#)]
108. Zhou, F.; Wang, P.; Chen, J.; Zhu, Z.; Li, Y.; Wang, S.; Wu, S.; Sima, Y.; Fu, T.; Tan, W.; et al. A photochemically covalent lock stabilizes aptamer conformation and strengthens its performance for biomedicine. *Nucleic Acids Res.* **2022**, *50*, 9039–9050. [[CrossRef](#)]
109. Xue, C.; Zhang, S.; Yu, X.; Hu, S.; Lu, Y.; Wu, Z.S. Periodically Ordered, Nuclease-Resistant DNA Nanowires Decorated with Cell-Specific Aptamers as Selective Theranostic Agents. *Angew. Chem. Int. Ed.* **2020**, *59*, 17540–17547. [[CrossRef](#)]

Disclaimer/Publisher's Note: The statements, opinions and data contained in all publications are solely those of the individual author(s) and contributor(s) and not of MDPI and/or the editor(s). MDPI and/or the editor(s) disclaim responsibility for any injury to people or property resulting from any ideas, methods, instructions or products referred to in the content.